

Hidden-charm pentaquarks and P_c states

Xin-Zhen Weng^{1,*}, Xiao-Lin Chen^{1,†}, Wei-Zhen Deng^{1,‡} and Shi-Lin Zhu^{1,2,3,§}

¹*School of Physics and State Key Laboratory of Nuclear Physics and Technology, Peking University, Beijing 100871, China*

²*Center of High Energy Physics, Peking University, Beijing 100871, China*

³*Collaborative Innovation Center of Quantum Matter, Beijing 100871, China*

Recently, the LHCb Collaboration reported three P_c states in the $J/\psi p$ channel. We systematically study the mass spectrum of the hidden charm pentaquark in the framework of an extended chromomagnetic model. For the $nnnc\bar{c}$ pentaquark with $I = 1/2$, we find that (i) the lowest state is $P_c(4327.0, 1/2, 1/2^-)$ [We use $P_c(m, I, J^P)$ to denote the $nnnc\bar{c}$ pentaquark], which corresponds to the $P_c(4312)$. Its dominant decay mode is $\Lambda_c \bar{D}^*$. (ii) We find two states in the vicinity of $P_c(4380)$. The first one is $P_c(4367.4, 1/2, 3/2^-)$ and decays dominantly to NJ/ψ and $\Lambda_c \bar{D}^*$. The other one is $P_c(4372.4, 1/2, 1/2^-)$. Its dominant decay mode is $\Lambda_c \bar{D}$, and its partial decay width of $N\eta_c$ channel is comparable to that of NJ/ψ . (iii) In higher mass region, we find $P_c(4476.3, 1/2, 3/2^-)$ and $P_c(4480.9, 1/2, 1/2^-)$, which correspond to $P_c(4440)$ and $P_c(4457)$. In the open charm channels, both of them decay dominantly to the $\Lambda_c \bar{D}^*$. (iv) We predict two states above 4.5 GeV, namely $P_c(4524.5, 1/2, 3/2^-)$ and $P_c(4546.0, 1/2, 5/2^-)$. The masses of the $nnnc\bar{c}$ state with $I = 3/2$ are all over 4.6 GeV. Moreover, we use the model to explore the $nns\bar{c}$, $ssn\bar{c}$, and $sss\bar{c}$ pentaquark states.

I. INTRODUCTION

Before the birth of quantum chromodynamics (QCD), the possible existence of tetraquark ($qq\bar{q}\bar{q}$) and pentaquark ($qqqq\bar{q}$) had been anticipated when Gell-Mann [1] and Zweig [2] first proposed the quark model. In 1976, Jaffe studied the light tetraquark in the framework of the MIT bag model [3, 4]. Chan and Högaasen also studied this topic in the color-magnetic spin-spin interaction from the one-gluon exchange [5]. Chao further considered the hidden-charm [6, 7] and full-charm [8] tetraquarks. Meanwhile, the pentaquark was also studied in many models, such as the color-magnetic hyperfine interaction [9, 10] and the MIT bag model [11].

In spite of the theoretical investigations, the first experimental evidence of the exotic states did not appear until 2003, when the Belle Collaboration observed the $X(3872)$ state in the exclusive $B^\pm \rightarrow K^\pm \pi^+ \pi^- J/\psi$ decays [12]. Later, the CDF [13], D0 [14], BABAR [15], LHCb [16], CMS [17], and BESIII [18] Collaborations confirmed this state, and the LHCb Collaboration further determined its quantum number to be $I^G J^{PC} = 0^+ 1^{++}$ [16]. For over a decade, lots of charmoniumlike XYZ states have been observed, such as $Y(3940)$ [19], $Y(4140)$ [20], $Y(4260)$ [21], $Y(4360)$ [22], $Y(4660)$ [23], and so on. Many of the XYZ states do not fit into the conventional $q\bar{q}$ meson spectrum in the quark model. To explain their nature, theorists have interpreted some of them to be the molecular state [24, 25], hybrid meson [26, 27], tetraquark [28, 29], etc. More detailed reviews can be found in Refs. [25, 30–34] and references therein.

Compared to the tetraquark candidates, the experimental observation of the pentaquark states is more difficult. In 2015, the LHCb Collaboration measured the $\Lambda_b \rightarrow J/\psi K^- p$ decays, and observed two resonances, $P_c(4380)$ and $P_c(4450)$, in the $J/\psi p$ channel, which indicates that they have a minimal quark content of $uudc\bar{c}$ [35]. Very recently, the LHCb Collaboration reported the observation of three narrow peaks in the $J/\psi p$ invariant mass spectrum of the $\Lambda_b \rightarrow J/\psi K p$ decays [36]. They found that the $P_c(4450)^+$ is actually composed of two narrow resonances, $P_c(4440)^+$ and $P_c(4457)^+$. Moreover, they also reported a new state below the $\Sigma_c \bar{D}$ threshold, namely the $P_c(4312)^+$. Their masses and widths are as follows:

$$\begin{aligned} P_c(4312)^+ : M &= 4311.9 \pm 0.7_{-0.6}^{+6.8} \text{ MeV}, \\ \Gamma &= 9.8 \pm 2.7_{-4.5}^{+3.7} \text{ MeV}, \\ P_c(4440)^+ : M &= 4440.3 \pm 1.3_{-4.7}^{+4.1} \text{ MeV}, \\ \Gamma &= 20.6 \pm 4.9_{-10.1}^{+8.7} \text{ MeV}, \\ P_c(4457)^+ : M &= 4457.3 \pm 0.6_{-1.7}^{+4.1} \text{ MeV}, \\ \Gamma &= 6.4 \pm 2.0_{-1.9}^{+5.7} \text{ MeV}. \end{aligned}$$

Since their masses are slightly below the $\Sigma_c \bar{D}$, $\Sigma_c^* \bar{D}$, and $\Sigma_c \bar{D}^*$ thresholds respectively, they can be interpreted as molecules composed of a charm baryon and an anticharm meson [37–49]. For example, Chen [46] interpreted them as bound states of $\Sigma_c \bar{D}$ with $J^P = 1/2^-$, $\Sigma_c^* \bar{D}$ with $J^P = 3/2^-$, and $\Sigma_c \bar{D}^*$ with $J^P = 3/2^-$, while Chen *et al.* [45], He [48], and Liu *et al.* [49] interpreted the $P_c(4312)$, $P_c(4440)$, and $P_c(4457)$ as loosely bound $\Sigma_c \bar{D}$ with ($I = 1/2, J^P = 1/2^-$), $\Sigma_c \bar{D}^*$ with ($I = 1/2, J^P = 1/2^-$), and $\Sigma_c \bar{D}^*$ with ($I = 1/2, J^P = 3/2^-$).

Another interesting possibility is that some of the P_c states might be tightly bound pentaquark states. The light $q^4 \bar{q}$ pentaquark states was first studied with the color-magnetic interaction among the quarks [9, 10]. Later, Strottman used the MIT bag model to discuss this

* xzhweng@pku.edu.cn

† chenxl@pku.edu.cn

‡ dwz@pku.edu.cn

§ zhysl@pku.edu.cn

system, where the mass spectra mostly depend on the chromomagnetic interaction between the quarks (or antiquark) [11]. The hidden-charm pentaquarks were also studied in constituent quark model [50–57].

The quark model is widely used to investigate the mass spectra of hadrons [1, 2, 58–65]. In the quark model, each quark (antiquark) carries the kinetic energy $\sqrt{p^2 + m^2}$. In the nonrelativistic limit, the kinetic energy reduces to $m + p^2/2m$, and the interquark potential contains the lattice QCD-inspired linear confinement interaction and the short-range one-gluon-exchange (OGE) interaction. Usually the OGE interaction consists of the spin-independent color Coulomb-type terms, the spin-spin chromomagnetic interaction, the tensor interaction, and the spin-orbit interactions etc.

We can use the chromomagnetic model to study the ground state hadrons [3, 4, 61, 66–71]. In the chromomagnetic model, the mass of the ground state hadrons consists of the effective quark masses and the chromomagnetic hyperfine interaction. This simple model reproduced the hyperfine splitting of hadrons quite well. Compared to the quark model, the chromoelectric interaction has been absorbed by the effective quark masses. However, the one-body effective quark masses are not enough to account for the two-body chromoelectric effects. In Ref. [72], Karliner *et al.* found that the color-related binding terms are needed when they considered the interactions between a heavy (anti-)quark and a strange (or heavy) quark. Similarly, Høgaasen *et al.* generalized the chromomagnetic model and included a chromoelectric term $H_{\text{CE}} = -\sum_{i,j} A_{ij} \tilde{\lambda}_i \cdot \tilde{\lambda}_j$ to study the hidden-beauty partners of the $X(3872)$ [73]. Note that in 1978, Fukugita *et al.* had already used the color and chromomagnetic interactions to investigate the pseudo-baryons [9]. Chan *et al.* also used these interactions to study the properties of di/triquarks, which are constituents of multiquarks [74].

In Ref. [75], we extended the chromomagnetic model and included the effect of color interaction. According to color algebra, we further introduced the quark pair mass parameters (m_{qq} and $m_{q\bar{q}}$) to account for both the effective quark masses (m_q) and the color interaction (A_{qq} and $A_{q\bar{q}}$) between the two quarks. Then we used this model to calculate the masses of multiheavy baryons. Our calculated mass of Ξ_{cc} , 3633.3 ± 9.3 MeV is very close to the LHCb's experiment $[3621.40 \pm 0.72(\text{stat.} \pm 0.27(\text{syst.}) \pm 0.14(\Lambda_c) \text{ MeV}]$ [76].

In this paper, we systematically study the mass spectrum of the $qqqc\bar{c}$ ($q = n, s$, and $n = u, d$) pentaquarks in the extended chromomagnetic model. In Sec. II we introduce the extended chromomagnetic model. In Sec. III A we present the model parameters. Then we calculate and discuss the numerical results in Sec. III B. We conclude in Sec. IV.

II. THE EXTENDED CHROMOMAGNETIC MODEL

In the chromomagnetic (CM) model, the mass of hadron is governed by the Hamiltonian [5, 61, 69–71]

$$H = \sum_i m_i - \sum_{i<j} v_{ij} \mathbf{S}_i \cdot \mathbf{S}_j \mathbf{F}_i \cdot \mathbf{F}_j, \quad (1)$$

where m_i is the i th constituent quark's (or antiquark's) effective mass, which includes the constituent quark mass, the kinetic energy, and so on, and $\mathbf{S}_i = \boldsymbol{\sigma}_i/2$ and $\mathbf{F}_i = \tilde{\boldsymbol{\lambda}}_i/2$ are the quark spin and color operators, respectively. For the antiquark, $\mathbf{S}_{\bar{q}} = -\mathbf{S}_q^*$ and $\mathbf{F}_{\bar{q}} = -\mathbf{F}_q^*$. The coefficient v_{ij} depends on the spatial wave function and the quark masses

$$v_{ij} = \frac{8\pi}{3m_i m_j} \langle \alpha_s(r) \delta^3(\mathbf{r}) \rangle. \quad (2)$$

As pointed out in Refs. [72, 73, 75], the effective quark masses are not enough to absorb all the two-body chromoelectric effects. To solve this problem, Høgaasen *et al.* generalized the chromomagnetic model by including a chromoelectric term [73]

$$H_{\text{CE}} = -\sum_{i,j} A_{ij} \tilde{\lambda}_i \cdot \tilde{\lambda}_j. \quad (3)$$

Since

$$\begin{aligned} & \sum_{i<j} (m_i + m_j) \mathbf{F}_i \cdot \mathbf{F}_j \\ &= \left(\sum_i m_i \mathbf{F}_i \right) \cdot \left(\sum_i \mathbf{F}_i \right) - \frac{4}{3} \sum_i m_i, \end{aligned} \quad (4)$$

and the total color operator $\sum_i \mathbf{F}_i$ nullifies any colorless physical state, we introduced a new quark pair mass parameter

$$m_{ij} = (m_i + m_j) + \frac{16}{3} A_{ij}, \quad (5)$$

and rewrite the model Hamiltonian as [75]

$$H_{\text{CM}} = -\frac{3}{4} \sum_{i<j} m_{ij} V_{ij}^{\text{C}} - \sum_{i<j} v_{ij} V_{ij}^{\text{CM}}, \quad (6)$$

where

$$V_{ij}^{\text{C}} = \mathbf{F}_i \cdot \mathbf{F}_j, \quad (7)$$

$$V_{ij}^{\text{CM}} = \mathbf{S}_i \cdot \mathbf{S}_j \mathbf{F}_i^a \cdot \mathbf{F}_j^a, \quad (8)$$

are the color and CM interactions between quarks.

To investigate the mass spectra of the pentaquark states, we need to construct the wave functions. A detailed construction of the pentaquark wave functions in the $(q_1 q_2 \otimes q_3) \otimes (q_4 \bar{q}_5)$ configuration can be found in Appendix A. Diagonalizing the Hamiltonian in these bases, we can obtain the mass spectrum and eigenvector of the hidden charm pentaquark states.

III. NUMERICAL RESULTS

A. Parameters

In Ref. [75], we have carefully extracted the parameters of the extended chromomagnetic model from the ground state mesons and baryons. Specifically, the parameters $m_{q\bar{q}}$ and $v_{q\bar{q}}$ are extracted from the mesons. The m_{qq} and v_{qq} with at most one heavy quark are extracted from the light and singly heavy baryons, and those with two heavy quarks are estimated from a quark model consideration. With these parameters, we calculated the mass of Ξ_{cc} to be 3633.3 ± 9.3 MeV, which is very close to the LHCb's result, $M_{\Xi_{cc}} = 3621.40 \pm 0.72$ MeV [76]. All parameters are listed in Table I. In this work, we use the same parameters to study the mass spectrum of the S -wave $qqq\bar{c}$ pentaquark states.

B. The hidden-charm pentaquarks

1. The $nnnc\bar{c}$ system

The calculated eigenvalues and eigenvectors of the $nnnc\bar{c}$ system are listed in Table II. First we consider the $nnnc\bar{c}$ state with isospin $I = 1/2$. The lowest state has mass of 3097.0 MeV with $J^P = 1/2^-$. This state, $\sum_i b_i \Psi_{D_i}^{1/2}$ with

$$\{b_i\} = \{0.111, -0.112, 0.013, 0.001, 0.987\}, \quad (9)$$

has a dominant component of $\Psi_{D_5}^{1/2}$. Notice that in the $nnn\otimes c\bar{c}$ configuration, $\Psi_{D_5}^{1/2}$ can be written as a direct product of a baryon and a meson,

$$\Psi_{D_5}^{1/2} = N \otimes \eta_c. \quad (10)$$

In other words, this state couples almost completely to the $N\eta_c$ scattering state. Therefore it has probably a very broad width and is just a part of the continuum. It is worth stressing that this kind of state also exists in the calculation of the $q\bar{q}c\bar{c}$ tetraquark, where the lowest state couples strongly to a heavy charmonium and a light meson [28, 77]. Moreover, the states of 4024.2 MeV (with $J^P = 1/2^-$) and 4028.2 MeV (with $J^P = 3/2^-$) couple strongly to N and J/ψ channel. The above states are also scattering states. We label these scattering states in the fifth column of Table II. The situation of the $nnnc\bar{c}$ states with $I = 3/2$ is similar. There are four low mass states. The lowest one, 4217.5 MeV with $J^P = 3/2^-$, is a scattering state of Δ and η_c , and the other three states, 4320.8 MeV with $J^P = 1/2^-$, 4336.0 MeV with $J^P = 3/2^-$ and 4336.8 MeV with $J^P = 3/2^-$, couple very strongly to Δ and J/ψ .

After identifying the scattering states, the other states are genuine pentaquarks. We plot their relative position in Fig. 1. For simplicity, we use $P_c(m, I, J^P)$ to denote the $nnnc\bar{c}$ pentaquark states. From Table II, we

see that the lightest state is $P_c(4327.0, 1/2, 1/2^-)$. This state is very close to the recently observed $P_c(4312)$. If the future experiment does confirm the quantum number of $P_c(4312)$ to be $1/2^-$, it is likely a tightly bound pentaquark state. We find two states in the vicinity of $P_c(4380)$, namely the $P_c(4367.4, 1/2, 3/2^-)$ and $P_c(4372.4, 1/2, 1/2^-)$. If $P_c(4380)$ truly corresponds to one of the two states, the other state should also exist, which can be searched for in future experiment. In higher energy region, we find the $P_c(4476.3, 1/2, 3/2^-)$ and $P_c(4480.9, 1/2, 1/2^-)$, which can be identified with $P_c(4440)$ and $P_c(4457)$ [36]. Above 4.5 GeV, there are $P_c(4524.5, 1/2, 3/2^-)$ and $P_c(4546.0, 1/2, 5/2^-)$. The $nnnc\bar{c}$ pentaquark with isospin $I = 3/2$ are all above 4.6 GeV.

Besides the mass spectrum, the eigenvectors also provide important information about the decay properties [3, 11, 53, 78]. We can calculate the overlap between the pentaquark and a particular baryon \times meson state. Then we can determine the decay amplitude of the pentaquark into that particular baryon \times meson channel. To calculate the overlap, we transform the eigenvectors of the pentaquark states into the $nnc\otimes n\bar{c}$ configuration (see Table XVI of Appendix B). Normally, the nnc and $n\bar{c}$ components inside the pentaquark can be either of color-singlet or of color-octet. The former one can easily dissociate into a S -wave meson and a S -wave baryon (the so-called ‘‘Okubo-Zweig-Iizuka (OZI)-superallowed’’ decays [3]). The latter one cannot fall apart without the gluon exchange. For simplicity, we follow Refs. [3, 11] and focus on the ‘‘OZI-superallowed’’ decays in this work. For the color-singlet part, we can rewrite the base states as a direct product of a baryon and a meson. For each decay mode, the branching fraction is proportional to the square of the coefficient of the corresponding component in the eigenvectors, and also depends on the phase space. For the two body L -wave decay, its partial width reads [79]

$$\Gamma_i = \gamma_i \alpha \frac{k^{2L+1}}{m^{2L}} \cdot |c_i|^2, \quad (11)$$

where α is an effective coupling constant, γ_i is a quantity determined by the decay dynamics, m is the mass of the parent particle, k is the momentum of the daughter particles in the rest frame of the parent particle, and c_i is the coefficient of the corresponding component. For the decay processes which we are interested in, $(k/m)^2$ is of $\mathcal{O}(10^{-2})$ or even smaller. Thus we only consider the S -wave decays since the higher wave decays are all suppressed. Next we have to estimate the γ_i . Generally, γ_i depends on the spatial wave functions of the initial pentaquark and final meson and baryon, which are different for each decay process. In the quark model, the spatial wave functions of the ground state scalar and vector meson are the same. And in the heavy quark limit, Σ_c and Σ_c^* have the same spatial wave function. Furthermore, the spatial wave function of Λ_c does not differ

TABLE I. Parameters of the $q\bar{q}$ and qq pairs (in units of MeV).

$m_{n\bar{n}}$	$m_{n\bar{s}}$	$m_{s\bar{s}}$	$m_{n\bar{c}}$	$m_{s\bar{c}}$	$m_{c\bar{c}}$	$m_{n\bar{b}}$	$m_{s\bar{b}}$	$m_{c\bar{b}}$	$m_{b\bar{b}}$
615.95	794.22	936.40	1973.22	2076.14	3068.53	5313.35	5403.25	6322.27	9444.97
$v_{n\bar{n}}$	$v_{n\bar{s}}$	$v_{s\bar{s}}$	$v_{n\bar{c}}$	$v_{s\bar{c}}$	$v_{c\bar{c}}$	$v_{n\bar{b}}$	$v_{s\bar{b}}$	$v_{c\bar{b}}$	$v_{b\bar{b}}$
477.92	298.57	249.18	106.01	107.87	85.12	33.89	36.43	47.18	45.98
m_{nn}	m_{ns}	m_{ss}	m_{nc}	m_{sc}	m_{cc}	m_{nb}	m_{sb}	m_{cb}	m_{bb}
724.85	906.65	1049.36	2079.96	2183.68	3171.51	5412.25	5494.80	6416.07	9529.57
v_{nn}	v_{ns}	v_{ss}	v_{nc}	v_{sc}	v_{cc}	v_{nb}	v_{sb}	v_{cb}	v_{bb}
305.34	212.75	195.30	62.81	70.63	56.75	19.92	8.47	31.45	30.65

TABLE II. Pentaquark masses and eigenvectors of the $nnnc\bar{c}$ system. The masses are all in units of MeV.

System	J^P	Mass	Eigenvector	Scattering state
$(nnnc\bar{c})^{I=3/2}$	$\frac{1}{2}^-$	4320.8	{0.070, -0.217, 0.974}	$\Delta J/\psi(4329)$
		4601.9	{0.733, -0.651, -0.197}	
		4717.1	{0.677, 0.727, 0.114}	
	$\frac{3}{2}^-$	4217.5	{-0.119, -0.016, -0.993}	$\Delta\eta_c(4216)$
		4336.0	{-0.052, -0.998, 0.022}	$\Delta J/\psi(4329)$
		4633.0	{0.992, -0.054, -0.118}	
$\frac{5}{2}^-$	4336.8	{1}	$\Delta J/\psi(4329)$	
$(nnnc\bar{c})^{I=1/2}$	$\frac{1}{2}^-$	3907.0	{0.111, -0.112, 0.013, 0.001, 0.987}	$N\eta_c(3923)$
		4024.2	{0.042, 0.042, 0.130, -0.990, -0.000}	$NJ/\psi(4036)$
		4327.0	{0.773, -0.356, 0.501, 0.084, -0.134}	
		4372.4	{0.189, 0.907, 0.358, 0.093, 0.077}	
		4480.9	{0.594, 0.193, -0.777, -0.069, -0.035}	
	$\frac{3}{2}^-$	4028.2	{0.035, 0.078, -0.032, -0.996}	$NJ/\psi(4036)$
		4367.4	{-0.570, -0.356, 0.737, -0.072}	
		4476.3	{0.819, -0.312, 0.482, -0.011}	
		4524.5	{0.057, 0.877, 0.473, 0.056}	
$\frac{5}{2}^-$	4546.0	{1}		

much from that of Σ_c . Then for each pentaquark,

$$\gamma_{\Delta J/\psi} = \gamma_{\Delta\eta_c}, \quad (12)$$

$$\gamma_{NJ/\psi} = \gamma_{N\eta_c}, \quad (13)$$

and

$$\gamma_{\Sigma_c^* \bar{D}^*} = \gamma_{\Sigma_c^* \bar{D}} = \gamma_{\Sigma_c \bar{D}^*} = \gamma_{\Sigma_c \bar{D}} \approx \gamma_{\Lambda_c \bar{D}^*} = \gamma_{\Lambda_c \bar{D}}. \quad (14)$$

The values of the relative widths of different decay modes are listed in Tables III and IV.

First we consider the $I = 1/2$ case. The lowest state, $P_c(4327.0, 1/2, 1/2^-)$, has two hidden charm decay modes, namely NJ/ψ and $N\eta_c$. Their partial decay

width ratio is

$$\frac{\Gamma[P_c(4327.0, 1/2, 1/2^-) \rightarrow N\eta_c]}{\Gamma[P_c(4327.0, 1/2, 1/2^-) \rightarrow NJ/\psi]} = 3.0, \quad (15)$$

which indicates that the partial decay width of the $N\eta_c$ channel is larger than that of the NJ/ψ . On the other hand, $P_c(4327.0, 1/2, 1/2^-)$ also has open charm decay modes. From Table IV, we see that $\Sigma_c \bar{D}$ and $\Lambda_c \bar{D}^*$ are its dominant decay modes. It is worth stressing that the calculated mass of this state is just several MeV higher than the threshold of $\Sigma_c \bar{D}$ (4321 MeV); considering the error of the model (Taking Ξ_{cc} for example, our calculation differs from the experiment by 12 MeV [75]), this state may probably lie below the $\Sigma_c \bar{D}$ threshold and

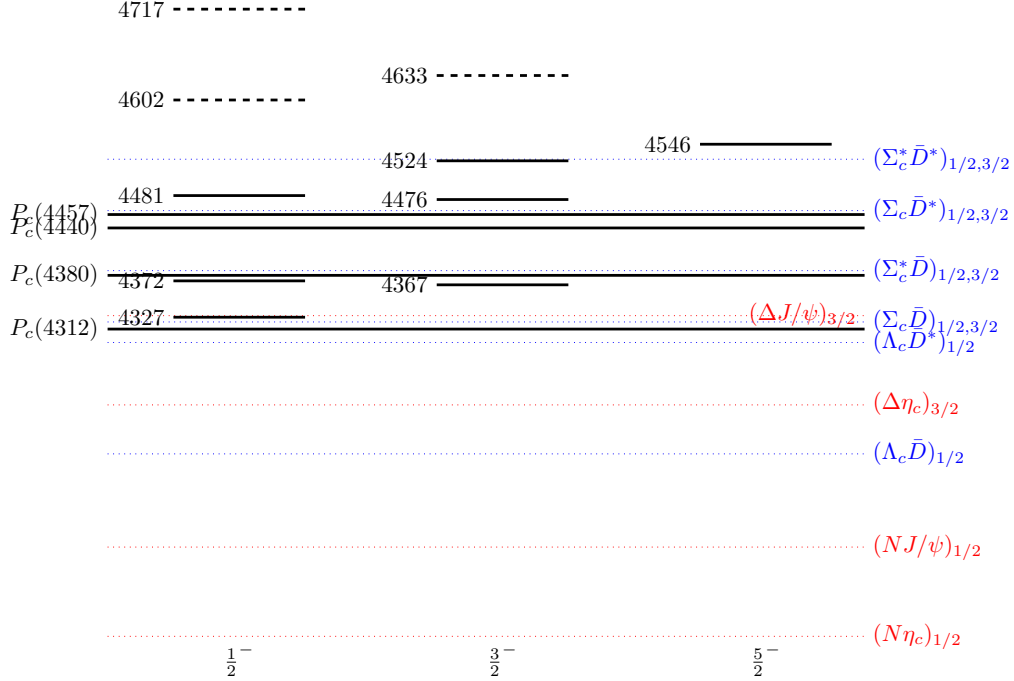


FIG. 1. Mass spectra of the $I = \frac{1}{2}$ (solid) and $I = \frac{3}{2}$ (dashed) $nnnc\bar{c}$ pentaquark states. The dotted lines indicate various meson-baryon thresholds and the long solid lines indicate the observed P_c states. The masses are all in units of MeV.

TABLE III. The partial width ratios for the hidden-charm decays of the $nnnc\bar{c}$ pentaquark states. For each state, we chose one mode as the reference channel, and the partial width ratios of the other channels are calculated relative to this channel. The masses are all in units of MeV.

I	J^P	Mass	$\Delta J/\psi$	$\Delta\eta_c$	NJ/ψ	$N\eta_c$
$\frac{3}{2}$	$\frac{1}{2}^-$	4601.9	1			
		4717.1	1			
	$\frac{3}{2}^-$	4633.0	1	5.5		
$\frac{1}{2}$	$\frac{1}{2}^-$	4327.0			1	3.0
		4372.4			1	0.8
		4480.9			1	0.3
	$\frac{3}{2}^-$	4367.4			1	
$\frac{3}{2}$	$\frac{3}{2}^-$	4476.3			1	
		4524.5			1	
	$\frac{5}{2}^-$	4546.0				

thus cannot decay into this channel. If we assume that the $P_c(4327.0, 1/2, 1/2^-)$ corresponds to the observed $P_c(4312)$ state, we have

$$\frac{\Gamma[P_c(4312) \rightarrow N\eta_c]}{\Gamma[P_c(4312) \rightarrow NJ/\psi]} = 3.1. \quad (16)$$

TABLE IV. The partial width ratios for the open charm decays of the $nnnc\bar{c}$ pentaquark states. For each state, we chose one mode as the reference channel, and the partial width ratios of other channels are calculated relative to this channel. The masses are all in units of MeV.

I	J^P	Mass	$\Sigma_c^* \bar{D}^*$	$\Sigma_c^* \bar{D}$	$\Sigma_c \bar{D}^*$	$\Sigma_c \bar{D}$	$\Lambda_c \bar{D}^*$	$\Lambda_c \bar{D}$
$\frac{3}{2}$	$\frac{1}{2}^-$	4601.9	0.05		1	0.4		
		4717.1	7.0		1	0.2		
	$\frac{3}{2}^-$	4633.0	5.3	3.1	1			
$\frac{1}{2}$	$\frac{1}{2}^-$	4327.0	0		0	1.3	1	0.02
		4372.4	0		0	0.7	1	57.6
		4480.9	0		0.3	0.09	1	0.07
	$\frac{3}{2}^-$	4367.4	0	0	0		1	
$\frac{3}{2}$	$\frac{3}{2}^-$	4476.3	0	0.2	1.9		1	
		4524.5	0	0.58	0.63		1	
	$\frac{5}{2}^-$	4546.0	1					

If the $P_c(4312)$ is observed in the $N\eta_c$ channel, and its partial decay width is larger than that of the NJ/ψ channel, then the $P_c(4312)$ is very likely a tightly bound pentaquark which corresponds the $P_c(4327.0, 1/2, 1/2^-)$. If the $P_c(4312)$ does not appear in the $N\eta_c$ channel, or its partial decay width is much smaller than that of the

NJ/ψ channel, the $P_c(4312)$ may not be a tightly bound pentaquark. Moreover,

$$\frac{\Gamma[P_c(4312) \rightarrow \Lambda_c \bar{D}]}{\Gamma[P_c(4312) \rightarrow \Lambda_c \bar{D}^*]} = 0.02. \quad (17)$$

We hope the future experiments can search for the $P_c(4312)$ in the $N\eta_c$ and $\Lambda_c \bar{D}^*$ channels.

Next we consider the two states in the vicinity of $P_c(4380)$. The $P_c(4367.4, 1/2, 3/2^-)$ only has one hidden charm decay mode NJ/ψ , while the $P_c(4372.4, 1/2, 1/2^-)$ can decay to both NJ/ψ and $N\eta_c$. Moreover,

$$\frac{\Gamma[P_c(4372.4, 1/2, 1/2^-) \rightarrow N\eta_c]}{\Gamma[P_c(4372.4, 1/2, 1/2^-) \rightarrow NJ/\psi]} = 0.8. \quad (18)$$

Thus this state can also be found in the $N\eta_c$ channel. On the other hand, $P_c(4367.4, 1/2, 3/2^-)$ can only decay to $\Lambda_c \bar{D}^*$, and $P_c(4372.4, 1/2, 1/2^-)$ decays dominantly to $\Lambda_c \bar{D}$.

Then we consider the $P_c(4476.3, 1/2, 3/2^-)$ and $P_c(4480.9, 1/2, 1/2^-)$. Both of them couple weakly to the hidden charm channel(s). Note that the former state can only decay to NJ/ψ while the latter state can also decay to $N\eta_c$, which can be used to distinguish the two states. In the open charm channels, both of the two states decay dominantly to the $\Lambda_c \bar{D}^*$ channel. The $\Sigma_c \bar{D}^*$ mode is also important for $P_c(4476.3, 1/2, 3/2^-)$. The mass difference between the $\Sigma_c \bar{D}^*$ threshold (4462 MeV) and the two states is only ~ 10 MeV, which is within the error of the CM model. The two states probably lie below the $\Sigma_c \bar{D}^*$ threshold and cannot decay through this mode. $P_c(4476.3, 1/2, 3/2^-)$ can also decay to $\Sigma_c^* \bar{D}$ with a not-so-small fraction. If $P_c(4476.3, 1/2, 3/2^-)$ and $P_c(4480.9, 1/2, 1/2^-)$ truly correspond to the $P_c(4440)$ and $P_c(4457)$ respectively, we have

$$\frac{\Gamma[P_c(4440) \rightarrow \Sigma_c^* \bar{D}]}{\Gamma[P_c(4440) \rightarrow \Lambda_c \bar{D}^*]} = 0.16, \quad (19)$$

$$\frac{\Gamma[P_c(4457) \rightarrow N\eta_c]}{\Gamma[P_c(4457) \rightarrow NJ/\psi]} = 0.29, \quad (20)$$

and

$$\begin{aligned} \Gamma[P_c(4457) \rightarrow \Sigma_c \bar{D}] : \Gamma[P_c(4457) \rightarrow \Lambda_c \bar{D}^*] \\ : \Gamma[P_c(4457) \rightarrow \Lambda_c \bar{D}] = 0.09 : 1 : 0.07. \end{aligned} \quad (21)$$

Finally, we consider the two states over 4.5 GeV. We see that $P_c(4524.5, 1/2, 3/2^-)$ may also be observed in the NJ/ψ channel, while $P_c(4546.0, 1/2, 5/2^-)$ can only decay to this mode through higher partial waves, which is suppressed. The dominant decay modes of $P_c(4524.5, 1/2, 3/2^-)$ are $\Sigma_c^* \bar{D}$, $\Sigma_c \bar{D}^*$ and $\Lambda_c \bar{D}^*$. Note that the $\Sigma_c^* \bar{D}$ mode has the largest coefficient in the eigenvector, but this mode is suppressed by phase space. And the $P_c(4546.0, 1/2, 5/2^-)$ can only decay to $\Sigma_c^* \bar{D}^*$.

There are three $nnnc\bar{c}$ pentaquark states with $I = 3/2$. Their masses are all above 4.6 GeV. Their couplings to $\Delta J/\psi$ are not very small (see Table II or see Table XVI of Appendix B), thus they can be observed in the $\Delta J/\psi$ channel in the future experiments. We also calculate the partial decay width ratio of each mode. For $P_c(4601.9, 3/2, 1/2^-)$ and $P_c(4717.1, 3/2, 1/2^-)$ states, we have

$$\Gamma_{\Sigma_c^* \bar{D}^*} : \Gamma_{\Sigma_c \bar{D}^*} : \Gamma_{\Sigma_c \bar{D}} = 0.05 : 1 : 0.4 \quad (22)$$

and

$$\Gamma_{\Sigma_c^* \bar{D}^*} : \Gamma_{\Sigma_c \bar{D}^*} : \Gamma_{\Sigma_c \bar{D}} = 7.0 : 1 : 0.2 \quad (23)$$

respectively. And for $P_c(4633.0, 3/2, 3/2^-)$, we have

$$\Gamma_{\Delta J/\psi} : \Gamma_{\Delta\eta_c} = 1 : 5.5 \quad (24)$$

and

$$\Gamma_{\Sigma_c^* \bar{D}^*} : \Gamma_{\Sigma_c^* \bar{D}} : \Gamma_{\Sigma_c \bar{D}^*} = 5.3 : 3.1 : 1. \quad (25)$$

In both cases, the P_c states have a large decay fraction to the open charm channels. Since all P_c states are observed in the NJ/ψ channel, it is very helpful if the future experiments can search for the open charm channels.

2. The $nmsc\bar{c}$ system

Now we turn to the $nmsc\bar{c}$ systems. The mass spectrum of the $nmsc\bar{c}$ system is listed in Table V. Similar to the $nnnc\bar{c}$ case, we first identify the scattering states composed of a nns baryon and a charmonium. For the $I = 0$ case, the $\Lambda \otimes \eta_c$ scattering state corresponds to the spin-1/2 state around 4086.1 MeV. The $\Lambda \otimes J/\psi$ scattering states can be of spin-1/2 and -3/2. The latter one has a mass 4209.5 MeV, while the former one is more complex. Actually, there are two states correspond to the spin-1/2 $\Lambda \otimes J/\psi$ scattering state. Their masses are 4197.4 MeV and 4208.6 MeV respectively. Since they all have large fractions of color-octet components (57% and 46%), we still consider them as pentaquarks. We also reproduce most of the scattering states with $I = 1$. The scattering state of $\Sigma^{(*)}$ and η_c has $J^P = 1/2^- (3/2^-)$ and mass 4145.5 MeV (4366.8 MeV). And the $\Sigma \otimes J/\psi$ scattering states can be of $J^P = 1/2^- (4264.9 \text{ MeV})$ and $J^P = 3/2^- (4269.7 \text{ MeV})$. We only reproduce two $\Sigma^* \otimes J/\psi$ scattering states, namely the $J^P = 1/2^-$ one with mass 4466.7 MeV and the $J^P = 5/2^-$ one with mass 4487.8 MeV. For the spin-3/2 $\Lambda \otimes J/\psi$ case, there are two $J^P = 3/2^-$ states couple strongly to $\Sigma^* \otimes J/\psi$. Their masses are 4485.9 MeV and 4488.4 MeV, respectively. They also have large fractions of color-octet components (37% and 62%). Thus we consider them as pentaquarks. For clarity, we add a fifth column in Table V to label these scattering states. In the following, we will use $P_{c,s}(m, I, J^P)$ to denote the $nmsc\bar{c}$ pentaquark states.

TABLE V. Pentaquark masses and eigenvectors of the $nnsc\bar{c}$ systems. The masses are all in units of MeV.

System	J^P	Mass	Eigenvectors	Scattering state	
$(nnsc\bar{c})^{I=1}$	$\frac{1}{2}^-$	4145.5	{0.095, -0.017, -0.170, 0.108, -0.020, -0.0002, 0.003, -0.975}	$\Sigma\eta_c(4177)$	
		4264.9	{0.037, 0.115, 0.079, 0.038, 0.135, 0.005, -0.979, -0.014}	$\Sigma J/\psi(4290)$	
		4442.8	{-0.122, 0.224, 0.837, -0.190, 0.351, 0.144, 0.134, -0.190}		
		4466.7	{-0.086, 0.199, 0.173, 0.043, -0.180, -0.942, 0.006, -0.033}	$\Sigma^* J/\psi(4481)$	
		4522.2	{-0.565, -0.169, -0.141, -0.760, -0.178, -0.008, -0.105, -0.108}		
		4612.6	{0.019, -0.437, 0.454, 0.188, -0.732, 0.138, -0.106, -0.034}		
		4696.3	{-0.621, 0.566, -0.084, 0.408, -0.260, 0.229, 0.017, -0.005}		
		4808.1	{-0.512, -0.598, 0.019, 0.412, 0.437, -0.140, -0.012, -0.007}		
		$\frac{3}{2}^-$	4269.7	{0.033, -0.057, -0.121, 0.040, -0.001, -0.004, 0.990}	$\Sigma J/\psi(4290)$
	4366.8	{-0.080, -0.020, -0.009, 0.128, -0.019, -0.988, -0.009}	$\Sigma^* \eta_c(4368)$		
	4485.9	{-0.183, 0.421, 0.232, -0.323, 0.789, -0.053, 0.072}			
	4488.4	{0.306, -0.570, -0.288, 0.343, 0.610, 0.023, -0.091}			
	4584.9	{-0.235, -0.680, 0.581, -0.375, -0.022, -0.021, 0.054}			
	4636.2	{-0.268, -0.171, -0.709, -0.625, -0.016, -0.048, -0.062}			
	4728.8	{0.859, 0.053, 0.094, -0.478, -0.062, -0.132, 0.004}			
	$\frac{5}{2}^-$	4487.8	{0.006, 0.99998}	$\Sigma^* J/\psi(4481)$	
	4644.3	{0.99998, -0.006}			
	$(nnsc\bar{c})^{I=0}$	$\frac{1}{2}^-$	4086.1	{-0.126, -0.059, 0.022, 0.146, 0.001, 0.002, 0.979}	$\Lambda\eta_c(4100)$
4197.4			{0.045, 0.350, 0.130, 0.547, 0.361, 0.652, -0.059}		
4208.6			{-0.038, 0.381, 0.250, 0.479, 0.136, -0.735, -0.057}		
4386.6			{-0.208, 0.102, -0.327, 0.435, -0.797, 0.095, -0.078}		
4465.0			{0.735, 0.323, -0.572, -0.036, 0.040, -0.091, 0.132}		
4489.6			{0.152, -0.763, -0.255, 0.502, 0.238, -0.112, -0.096}		
4607.0			{0.612, -0.179, 0.649, 0.085, -0.397, 0.076, 0.041}		
$\frac{3}{2}^-$			4209.5	{0.041, 0.088, 0.024, -0.033, 0.994}	$\Lambda J/\psi(4212)$
4387.3			{0.101, 0.074, -0.402, -0.906, -0.031}		
4501.5		{0.521, 0.335, 0.743, -0.242, -0.077}			
4603.6		{-0.845, 0.258, 0.396, -0.249, -0.006}			
4656.0		{0.037, 0.899, -0.360, 0.239, -0.065}			
$\frac{5}{2}^-$		4680.6	{1}		

In Fig. 2, we show the relative position of the $nnsc\bar{c}$ pentaquark states. We also plot all the meson-baryon thresholds which they can decay to through quark rearrangement. Compared to the $nnnc\bar{c}$ case, the $nnsc\bar{c}$ system has larger numbers of states and decay patterns. There are 18 channels that the $nnsc\bar{c}$ pentaquarks may decay to. From the figure, we can easily identify the decay constrains of the isospin conservation and kinetics. Next we study their decay properties. Similar to the $nnnc\bar{c}$ case, we need to consider the γ_i . In the quark model, the spatial wave functions of the ground state

scalar and vector meson are the same. And the same spatial wave function of Σ^* does not differ much from that of Σ . In the heavy quark limit, Σ_c and Σ_c^* have the same spatial wave function. Similarly, the Ξ_c^* and Ξ_c' have the same spatial wave function, and their spatial wave functions do not differ much from that of Ξ_c . Thus for each $nnsc\bar{c}$ pentaquark

$$\gamma_{\Sigma^* J/\psi} = \gamma_{\Sigma^* \eta_c} \approx \gamma_{\Sigma J/\psi} = \gamma_{\Sigma \eta_c}, \quad (26)$$

$$\gamma_{\Lambda J/\psi} = \gamma_{\Lambda \eta_c}, \quad (27)$$

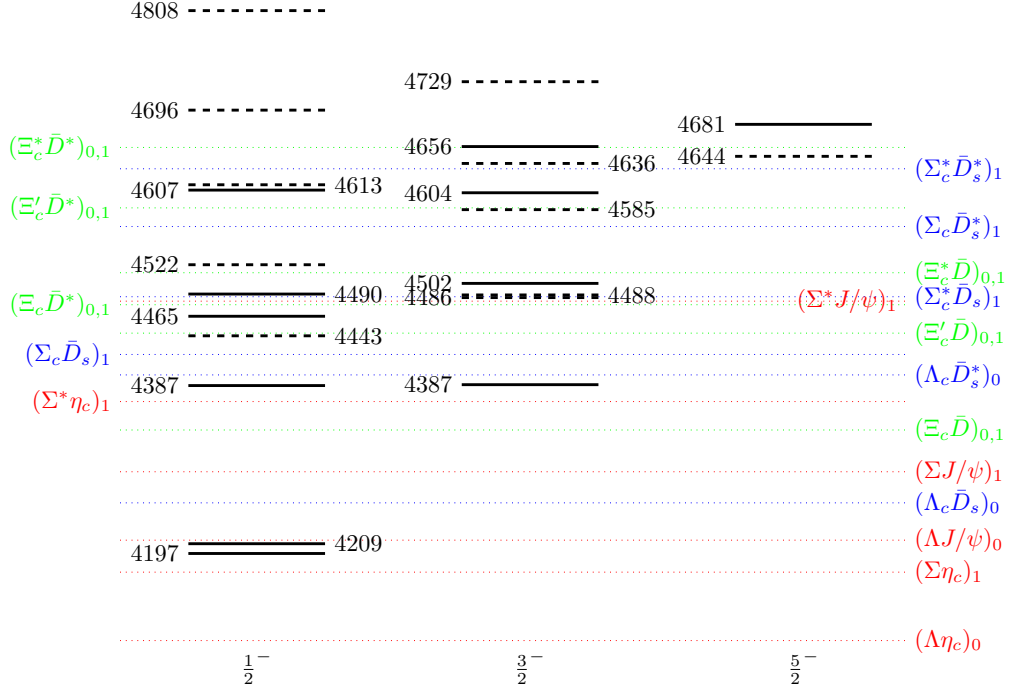


FIG. 2. Mass spectra of the $I = 0$ (solid) and $I = 1$ (dashed) $nnscc\bar{c}$ pentaquark states. The dotted lines indicate various meson-baryon thresholds. The masses are all in units of MeV.

$$\gamma_{\Sigma_c^* \bar{D}_s^*} = \gamma_{\Sigma_c^* \bar{D}_s} = \gamma_{\Sigma_c \bar{D}_s^*} = \gamma_{\Sigma_c \bar{D}_s}, \quad (28)$$

$$\gamma_{\Lambda_c \bar{D}_s^*} = \gamma_{\Lambda_c \bar{D}_s}, \quad (29)$$

and

$$\gamma_{\Xi_c^* \bar{D}^*} = \gamma_{\Xi_c^* \bar{D}} = \gamma_{\Xi_c' \bar{D}^*} = \gamma_{\Xi_c' \bar{D}} \approx \gamma_{\Xi_c \bar{D}^*} = \gamma_{\Xi_c \bar{D}}. \quad (30)$$

Combining the eigenvectors in the $nmc \otimes s\bar{c}$ and $nsc \otimes n\bar{c}$ configurations (see Tables XVII–XVIII of Appendix B), we can calculate the relative partial widths of different decay modes, as listed in Tables VI–VIII.

From the eigenvectors, we find a new type of scattering state, which consists of a charm baryon plus an anticharm meson. The $P_{c,s}(4584.9, 1, 3/2^-)$ has 82% of the $\Sigma_c \bar{D}_s^*$ component, while both the $P_{c,s}(4636.2, 1, 3/2^-)$ and $P_{c,s}(4644.3, 1, 5/2^-)$ have more than 85% of the $\Sigma_c^* \bar{D}_s^*$ component. Some other states, namely the $P_{c,s}(4386.6, 0, 1/2^-)$, $P_{c,s}(4387.3, 0, 3/2^-)$, $P_{c,s}(4680.6, 0, 5/2^-)$ and $P_{c,s}(4442.8, 1, 1/2^-)$ states, also have quite large fractions of the color-singlet open charm components. They are expected to be broad. But we still cannot rule out the possibility that they are pentaquark states. To obtain a more definite conclusion, one needs to consider the dynamics inside the pentaquark, which is beyond the present work.

Two of the lowest $nnscc\bar{c}$ pentaquark states are the $P_{c,s}(4197.4, 0, 1/2^-)$ and $P_{c,s}(4208.6, 0, 1/2^-)$. From Fig. 2, we see that they can only decay to $\Lambda\eta_c$, thus they

should have narrow widths. However, their wave functions have large overlaps with the $\Lambda J/\psi$, and their predicted masses are just below the $\Lambda J/\psi$ threshold. Considering the error of the present model, their masses can probably be larger than the $\Lambda J/\psi$ threshold. In that case, they will decay easily to $\Lambda J/\psi$ and be broader. Both $P_{c,s}(4386.6, 0, 1/2^-)$ and $P_{c,s}(4387.3, 0, 3/2^-)$ decay dominantly to $\Lambda J/\psi$. But $P_{c,s}(4386.6, 0, 1/2^-)$ can also decay to $\Lambda\eta_c$, with

$$\frac{\Gamma[P_{c,s}(4386.6, 0, 1/2^-) \rightarrow \Lambda\eta_c]}{\Gamma[P_{c,s}(4386.6, 0, 1/2^-) \rightarrow \Lambda J/\psi]} = 0.87. \quad (31)$$

The $P_{c,s}(4465.0, 0, 1/2^-)$ and $P_{c,s}(4489.6, 0, 1/2^-)$ have the same quantum numbers and decay channels, but we can still use their relative size of partial decay widths to distinguish them. For $P_{c,s}(4465.0, 0, 1/2^-)$, we have

$$\Gamma_{\Lambda J/\psi} : \Gamma_{\Lambda\eta_c} = 1 : 2.6, \quad (32)$$

$$\Gamma_{\Lambda_c \bar{D}_s^*} : \Gamma_{\Lambda_c \bar{D}_s} = 1 : 0.03, \quad (33)$$

and

$$\Gamma_{\Xi_c' \bar{D}} : \Gamma_{\Xi_c \bar{D}^*} : \Gamma_{\Xi_c \bar{D}} = 1 : 0 : 7.9. \quad (34)$$

And the $P_{c,s}(4489.6, 0, 1/2^-)$ has

$$\Gamma_{\Lambda J/\psi} : \Gamma_{\Lambda\eta_c} = 1 : 0.87, \quad (35)$$

TABLE VI. The partial width ratios for the hidden-charm decays of the $nnsc\bar{c}$ pentaquark states. The masses are all in units of MeV.

I	J^P	Mass	$\Sigma^* J/\psi$	$\Sigma^* \eta_c$	$\Sigma J/\psi$	$\Sigma \eta_c$	$\Lambda J/\psi$	$\Lambda \eta_c$
1	$\frac{1}{2}^-$	4442.8	0		1	2.7		
		4522.2	0.002		1	1.3		
	4612.6	1.1		1	0.12			
	4696.3	1		0.008	0.0008			
	4808.1	1		0.009	0.003			
	$\frac{3}{2}^-$	4485.9	18.5	0.4	1			
4488.4		8.6	0.05	1				
4584.9		0.10	0.14	1				
4636.2		0.05	0.54	1				
4728.8		1	5.5	0.007				
$\frac{5}{2}^-$		4644.3	1					
0	$\frac{1}{2}^-$	4197.4					0	1
		4208.6					0	1
		4386.6					1	0.87
		4465.0					1	2.6
		4489.6					1	0.87
		4607.0					1	0.33
$\frac{3}{2}^-$	4387.3					1		
	4501.5					1		
	4603.6					1		
	4656.0					1		
$\frac{5}{2}^-$	4680.6							

$$\Gamma_{\Lambda_c \bar{D}_s^*} : \Gamma_{\Lambda_c \bar{D}_s} = 1 : 134.1, \quad (36)$$

and

$$\Gamma_{\Xi_c \bar{D}} : \Gamma_{\Xi_c \bar{D}^*} : \Gamma_{\Xi_c \bar{D}} = 1 : 0.57 : 1.1. \quad (37)$$

Its dominant decay mode is $\Lambda_c \bar{D}_s$. For the $P_{c,s}$ (4501.5, 0, 3/2⁻), its dominant decay modes are $\Lambda_c \bar{D}_s^*$ and $\Xi_c \bar{D}^*$. It can also decay to $\Lambda J/\psi$. We also obtain three states above 4.6 GeV. We further study the $I = 1$ $nnsc\bar{c}$ pentaquark states. Their partial decay width ratios are also listed in Tables VI–VIII. There are three states above all meson-baryon thresholds [$P_{c,s}$ (4680.6, 0, 5/2⁻) is not included since it is a scattering state; see Fig. 2]. They may be broad since they can decay freely to many open charm channels.

Experimentally, three P_c states have been observed in the NJ/ψ channel. It is quite possible that the $P_{c,s}$ states can be found in the $\Lambda J/\psi$ and $\Sigma^{(*)} J/\psi$ channels. Moreover, we can also use open charm channels to search for these states.

TABLE VII. The partial width ratios for the $nnsc\bar{c}$ open charm decays of the $nnsc\bar{c}$ pentaquark states. The masses are all in units of MeV.

I	J^P	Mass	$\Sigma_c^* \bar{D}_s^*$	$\Sigma_c^* \bar{D}_s$	$\Sigma_c \bar{D}_s^*$	$\Sigma_c \bar{D}_s$	$\Lambda_c \bar{D}_s^*$	$\Lambda_c \bar{D}_s$
1	$\frac{1}{2}^-$	4442.8	0		0	1		
		4522.2	0		0	1		
	4612.6	0		1	0.0001			
	4696.3	0.00002		1.9	1			
	4808.1	37.7		5.6	1			
	$\frac{3}{2}^-$	4485.9	0	0	0			
4488.4		0	1	0				
4584.9		0	1	176.1				
4636.2		17.9	1	0.33				
4728.8		0.65	1	0.21				
$\frac{5}{2}^-$		4644.3	1					
0	$\frac{1}{2}^-$	4197.4					0	0
		4208.6					0	0
		4386.6					0	1
		4465.0					1	0.03
		4489.6					1	134.1
		4607.0					13.1	1
$\frac{3}{2}^-$	4387.3					0		
	4501.5					1		
	4603.6					1		
	4656.0					1		
$\frac{5}{2}^-$	4680.6							

3. The $ssnc\bar{c}$ and $sssc\bar{c}$ systems

The $ssnc\bar{c}$ system is similar to the $I = 1$ $nnsc\bar{c}$ system. We present their mass spectra in Table IX. As indicated in the last column, we reproduce the scattering states of $\Xi \eta_c$ (4288.0 MeV with $J^P = 1/2^-$), $\Xi J/\psi$ (4406.0 MeV with $J^P = 1/2^-$ and 4413.7 MeV with $J^P = 3/2^-$), $\Xi^* \eta_c$ (4509.4 MeV with $J^P = 3/2^-$) and $\Xi^* J/\psi$ (4604.7 MeV with $J^P = 1/2^-$, 4630.6 MeV with $J^P = 3/2^-$ and 4631.7 MeV with $J^P = 5/2^-$). In the following, we will use $P_{c,ss}(m, J^P)$ to denote the $ssnc\bar{c}$ pentaquark.

We plot the relative position of the $ssnc\bar{c}$ pentaquark states and all the relevant meson-baryon thresholds in Fig. 3. We also transform the eigenvectors to the $ssc\bar{c}$ and $nsc\bar{c}$ configurations (see Table XIX of Appendix B). The only state with $J^P = 5/2^-$, $P_{c,ss}(4790.0, 5/2^-)$, lies over all thresholds and

$$P_{c,ss}(4790.0, 5/2^-) = 0.94487 \Omega_c^* \bar{D}^* + \dots \quad (38)$$

It is a scattering state of $\Omega_c^* \bar{D}^*$. Its dominant decay mode



FIG. 3. Mass spectra of the $ss\bar{c}\bar{c}$ pentaquark states. The dotted lines indicate various meson-baryon thresholds. The masses are all in units of MeV.

is $\Omega_c^* \bar{D}^*$ and it should be broad. Similar to the $nn\bar{c}\bar{c}$ and $nn\bar{s}\bar{c}$, for each $ss\bar{c}\bar{c}$ pentaquark state,

$$\gamma_{\Xi^* J/\psi} = \gamma_{\Xi^* \eta_c} = \gamma_{\Xi J/\psi} = \gamma_{\Xi \eta_c}, \quad (39)$$

$$\gamma_{\Omega_c^* \bar{D}^*} = \gamma_{\Omega_c^* \bar{D}} = \gamma_{\Omega_c \bar{D}^*} = \gamma_{\Omega_c \bar{D}}, \quad (40)$$

$$\gamma_{\Xi_c^* \bar{D}_s^*} = \gamma_{\Xi_c^* \bar{D}_s} = \gamma_{\Xi_c' \bar{D}_s^*} = \gamma_{\Xi_c' \bar{D}_s} \approx \gamma_{\Xi_c \bar{D}_s^*} = \gamma_{\Xi_c \bar{D}_s}. \quad (41)$$

The calculated partial decay width ratios are listed in Tables X–XII.

The last class of the hidden-charm pentaquark is the $ss\bar{s}\bar{c}$ system. They are similar to the $nn\bar{c}\bar{c}$ states with isospin $I = 3/2$. We present their mass spectra in Table XIII. We find three scattering states (4736.0 MeV with $J^P = 1/2^-$, 4767.5 MeV with $J^P = 3/2^-$ and 4768.6 MeV with $J^P = 5/2^-$) which couple very strongly to the $\Omega J/\psi$ and a scattering state (4645.1 MeV with $J^P = 3/2^-$) which couples strongly to the $\Omega \eta_c$. We will focus on the other $ss\bar{s}\bar{c}$ pentaquark states. To study their decay properties, we transform their wave functions to the $ssc\bar{s}\bar{c}$ configuration (see Table XX of Appendix B). And we also plot their relative position in Fig. 4, along with all possible decay channels. We find that they are all above the open charm thresholds and have large overlap with the $\Omega_c^{(*)} \otimes \bar{D}_s^{(*)}$ component. Thus

they should all be very broad. The partial decay width ratios can be found in Tables XIV–XV.

IV. CONCLUSIONS

In this work, we have systematically studied the mass spectrum of the hidden charm pentaquark in the framework of an extended chromomagnetic model. In addition to the chromomagnetic interaction, the effect of color interaction is also considered in this model. With the eigenvectors obtained, we have further investigated the decay properties of the pentaquarks.

For the $nn\bar{c}\bar{c}$ pentaquark with $I = 1/2$, we find that the masses of the experimentally observed P_c states are compatible with such pentaquark states. The lowest state $P_c(4327.0, 1/2, 1/2^-)$ corresponds to the $P_c(4312)$. This state has two hidden charm channels, namely the NJ/ψ and $N\eta_c$ channels. And its partial decay width of the $N\eta_c$ mode is larger than that of the NJ/ψ mode. In the open charm decay channel, $P_c(4327.0, 1/2, 1/2^-)$ decays dominantly to the $\Lambda_c \bar{D}^*$ mode. We hope the future experiments can search for the $P_c(4312)$ in the $N\eta_c$ and $\Lambda_c \bar{D}^*$ channels.

There are two states, $P_c(4367.4, 1/2, 3/2^-)$ and $P_c(4372.4, 1/2, 1/2^-)$, in the vicinity of the $P_c(4380)$. $P_c(4367.4, 1/2, 3/2^-)$ decays into the NJ/ψ and $\Lambda_c \bar{D}^*$



FIG. 4. Mass spectra of the $sssc\bar{c}$ pentaquark states. The dotted lines indicate various meson-baryon thresholds. The masses are all in units of MeV.

modes, while the other hidden-charm (like $N\eta_c$) or open charm decay modes are all suppressed. Its partner state, $P_c(4372.4, 1/2, 1/2^-)$ can decay into both NJ/ψ and $N\eta_c$ modes. And their partial decay widths are comparable. In the open charm channel, $P_c(4372.4, 1/2, 1/2^-)$ decays dominantly to the $\Lambda_c\bar{D}$ mode. If $P_c(4380)$ truly corresponds to the $P_c(4367.4, 1/2, 3/2^-)$, this partner state should also exist, which can be searched for in future experiments.

In the higher mass region, we find $P_c(4476.3, 1/2, 3/2^-)$ and $P_c(4480.9, 1/2, 1/2^-)$. They may correspond to the $P_c(4440)$ and $P_c(4457)$, respectively. Both of them couple weakly to the hidden charm channel(s). Note that the former state can only decay to NJ/ψ while the latter state can also decay to $N\eta_c$, which can be used to distinguish the two states. In the open charm channels, both of them decay dominantly to the $\Lambda_c\bar{D}^*$. And the $P_c(4476.3, 1/2, 3/2^-)$ can also decay to $\Sigma_c^*\bar{D}$ with a not-so-small fraction.

Moreover, we predict two states above 4.5 GeV, namely $P_c(4524.5, 1/2, 3/2^-)$ and $P_c(4546.0, 1/2, 5/2^-)$. Like the observed P_c states, $P_c(4524.5, 1/2, 3/2^-)$ can also be observed in the NJ/ψ channel. In the open charm channel, it decays dominantly into $\Lambda_c\bar{D}^*$, while the $\Sigma_c^*\bar{D}$, $\Sigma_c\bar{D}^*$ modes are also important. On the other hand, $P_c(4546.0, 1/2, 5/2^-)$ can only decay to $\Sigma_c^*\bar{D}^*$, all other decay modes are suppressed.

There are three $nnnc\bar{c}$ pentaquark states with $I = 3/2$, their masses are all over 4.6 GeV. They can decay into the $\Delta J/\psi$ channel, while $P_c(4633.0, 3/2, 3/2^-)$ can also decays to $\Delta\eta_c$. In the open charm channel, $P_c(4601.9, 3/2, 1/2^-)$ decays dominantly to the $\Sigma_c\bar{D}^*$ and $\Sigma_c\bar{D}$ modes, $P_c(4717.1, 3/2, 1/2^-)$ decays dominantly to the $\Sigma_c^*\bar{D}^*$ and $\Sigma_c\bar{D}^*$ modes, and $P_c(4633.0, 3/2, 3/2^-)$ can decay to the $\Sigma_c^*\bar{D}^*$, $\Sigma_c^*\bar{D}$, and $\Sigma_c\bar{D}^*$ modes.

We have also used this model to explore the $nns\bar{c}$, $ssnc\bar{c}$, and $sssc\bar{c}$ pentaquark states. With the obtained eigenvectors, we further explore the hidden and open charm decays of these pentaquark states. We hope that future experiments in LHCb and other collaborations can search for these states.

ACKNOWLEDGMENTS

X. Z. W. is grateful to G. J. Wang and L. Meng for helpful comments and discussions. This project is supported by the National Natural Science Foundation of China under Grants No. 11575008, No. 11621131001 and National Key Basic Research Program of China (2015CB856700).

TABLE VIII. The partial width ratios for the $nsc\bar{c}\bar{n}$ open charm decays of the $nnsc\bar{c}$ pentaquark states. The masses are all in units of MeV.

I	J^P	Mass	$\Xi_c^* \bar{D}^*$	$\Xi_c^* \bar{D}$	$\Xi_c' \bar{D}^*$	$\Xi_c' \bar{D}$	$\Xi_c \bar{D}^*$	$\Xi_c \bar{D}$	
1	$\frac{1}{2}^-$	4442.8	0		0	0	0	1	
		4522.2	0		0	2.6	0.006	1	
		4612.6	0		2.2	0.24	3.4	1	
		4696.3	0.14		0.27	0.21	4.6	1	
		4808.1	151.4		7.4	5.0	12.8	1	
	$\frac{3}{2}^-$	4485.9	0	0	0			1	
		4488.4	0	0	0			1	
		4584.9	0	0.007	0			1	
		4636.2	0	0.38	0.49			1	
		4728.8	14.6	8.0	3.4			1	
0	$\frac{5}{2}^-$	4644.3	0						
		$\frac{1}{2}^-$	4197.4	0		0	0	0	0
			4208.6	0		0	0	0	0
			4386.6	0		0	0	0	1
			4465.0	0		0	1	0	7.9
	4489.6		0		0	0.88	0.50	1	
	4607.0	0		7.4	1.6	2.4	1		
	$\frac{3}{2}^-$	4387.3	0	0	0			0	
		4501.5	0	0	0			1	
		4603.6	0	1	0.35			18.0	
		4656.0	0.87	1	1.3			0.65	
		$\frac{5}{2}^-$	4680.6	1					

Appendix A: The pentaquark wave functions

In this section, we construct the pentaquark wave functions in the $(q_1 q_2 \otimes q_3) \otimes (q_4 \bar{q}_5)$ configuration. In principle, the total wave function is a direct product of the orbital, color, spin and flavor bases. Since we only consider the ground states, the orbital wave function is symmetric and irrelevant for the effective Hamiltonian [see Eq. (6)]. Moreover, the Hamiltonian does not contain a flavor operator explicitly. Thus we first construct the color-spin wave function, and then incorporate the flavor wave function to account for the Pauli principle.

The spins of the pentaquark states can be $1/2$, $3/2$, and $5/2$. In the $(qq \otimes q) \otimes q \bar{q}$ configuration, the possible color-spin wave functions are listed as follows,

1. $J^P = 1/2^-$:

$$\beta_1^{1/2} = |[(q_1 q_2)_1^6 q_3]_{3/2}^8 (q_4 \bar{q}_5)_1^8\rangle_{1/2},$$

$$\beta_2^{1/2} = |[(q_1 q_2)_1^6 q_3]_{1/2}^8 (q_4 \bar{q}_5)_1^8\rangle_{1/2},$$

$$\beta_3^{1/2} = |[(q_1 q_2)_0^6 q_3]_{1/2}^8 (q_4 \bar{q}_5)_1^8\rangle_{1/2},$$

$$\beta_4^{1/2} = |[(q_1 q_2)_1^6 q_3]_{1/2}^8 (q_4 \bar{q}_5)_0^8\rangle_{1/2},$$

$$\beta_5^{1/2} = |[(q_1 q_2)_0^6 q_3]_{1/2}^8 (q_4 \bar{q}_5)_0^8\rangle_{1/2},$$

$$\beta_6^{1/2} = |[(q_1 q_2)_1^3 q_3]_{3/2}^8 (q_4 \bar{q}_5)_1^8\rangle_{1/2},$$

$$\beta_7^{1/2} = |[(q_1 q_2)_1^3 q_3]_{1/2}^8 (q_4 \bar{q}_5)_1^8\rangle_{1/2},$$

$$\beta_8^{1/2} = |[(q_1 q_2)_0^3 q_3]_{1/2}^8 (q_4 \bar{q}_5)_1^8\rangle_{1/2},$$

$$\beta_9^{1/2} = |[(q_1 q_2)_1^3 q_3]_{1/2}^8 (q_4 \bar{q}_5)_0^8\rangle_{1/2},$$

$$\beta_{10}^{1/2} = |[(q_1 q_2)_0^3 q_3]_{1/2}^8 (q_4 \bar{q}_5)_0^8\rangle_{1/2},$$

$$\beta_{11}^{1/2} = |[(q_1 q_2)_1^3 q_3]_{3/2}^1 (q_4 \bar{q}_5)_1^1\rangle_{1/2},$$

$$\beta_{12}^{1/2} = |[(q_1 q_2)_1^3 q_3]_{1/2}^1 (q_4 \bar{q}_5)_1^1\rangle_{1/2},$$

$$\beta_{13}^{1/2} = |[(q_1 q_2)_0^3 q_3]_{1/2}^1 (q_4 \bar{q}_5)_1^1\rangle_{1/2},$$

$$\beta_{14}^{1/2} = |[(q_1 q_2)_1^3 q_3]_{1/2}^1 (q_4 \bar{q}_5)_0^1\rangle_{1/2},$$

$$\beta_{15}^{1/2} = |[(q_1 q_2)_0^3 q_3]_{1/2}^1 (q_4 \bar{q}_5)_0^1\rangle_{1/2}, \quad (\text{A1})$$

2. $J^P = 3/2^-$:

$$\beta_1^{3/2} = |[(q_1 q_2)_1^6 q_3]_{3/2}^8 (q_4 \bar{q}_5)_1^8\rangle_{3/2},$$

$$\beta_2^{3/2} = |[(q_1 q_2)_1^6 q_3]_{3/2}^8 (q_4 \bar{q}_5)_0^8\rangle_{3/2},$$

$$\beta_3^{3/2} = |[(q_1 q_2)_0^6 q_3]_{1/2}^8 (q_4 \bar{q}_5)_1^8\rangle_{3/2},$$

$$\beta_4^{3/2} = |[(q_1 q_2)_0^6 q_3]_{1/2}^8 (q_4 \bar{q}_5)_0^8\rangle_{3/2},$$

$$\beta_5^{3/2} = |[(q_1 q_2)_1^3 q_3]_{3/2}^8 (q_4 \bar{q}_5)_1^8\rangle_{3/2},$$

$$\beta_6^{3/2} = |[(q_1 q_2)_1^3 q_3]_{3/2}^8 (q_4 \bar{q}_5)_0^8\rangle_{3/2},$$

$$\beta_7^{3/2} = |[(q_1 q_2)_1^3 q_3]_{1/2}^8 (q_4 \bar{q}_5)_1^8\rangle_{3/2},$$

$$\beta_8^{3/2} = |[(q_1 q_2)_0^3 q_3]_{1/2}^8 (q_4 \bar{q}_5)_1^8\rangle_{3/2},$$

$$\beta_9^{3/2} = |[(q_1 q_2)_1^3 q_3]_{3/2}^1 (q_4 \bar{q}_5)_1^1\rangle_{3/2},$$

$$\beta_{10}^{3/2} = |[(q_1 q_2)_1^3 q_3]_{3/2}^1 (q_4 \bar{q}_5)_0^1\rangle_{3/2},$$

$$\beta_{11}^{3/2} = |[(q_1 q_2)_1^3 q_3]_{1/2}^1 (q_4 \bar{q}_5)_1^1\rangle_{3/2},$$

$$\beta_{12}^{3/2} = |[(q_1 q_2)_0^3 q_3]_{1/2}^1 (q_4 \bar{q}_5)_1^1\rangle_{3/2}, \quad (\text{A2})$$

3. $J^P = 5/2^-$:

$$\beta_1^{5/2} = |[(q_1 q_2)_1^6 q_3]_{3/2}^8 (q_4 \bar{q}_5)_1^8\rangle_{5/2},$$

$$\beta_2^{5/2} = |[(q_1 q_2)_1^3 q_3]_{3/2}^8 (q_4 \bar{q}_5)_1^8\rangle_{5/2},$$

$$\beta_3^{5/2} = |[(q_1 q_2)_1^3 q_3]_{3/2}^1 (q_4 \bar{q}_5)_1^1\rangle_{5/2}, \quad (\text{A3})$$

where the superscript 1, $\bar{3}$, 6, or 8 denotes the color, and the subscript denotes the spin 0, 1, $1/2$, $3/2$, or $5/2$.

TABLE IX. Pentaquark masses and eigenvectors of the $ssnc\bar{c}$ systems. The masses are all in units of MeV.

System	J^P	Mass	Eigenvector	Scattering state	
$ssnc\bar{c}$	$\frac{1}{2}^-$	4288.0	{0.123, -0.021, -0.169, 0.115, -0.019, -0.0001, 0.003, -0.971}	$\Xi\eta_c(4302)$	
		4406.0	{-0.043, -0.160, -0.095, -0.043, -0.146, 0.004, 0.969, 0.015}	$\Xi J/\psi(4415)$	
		4573.4	{0.222, -0.379, -0.781, 0.179, -0.303, 0.068, -0.171, 0.199}		
		4604.7	{-0.050, 0.239, -0.087, 0.130, -0.231, -0.928, 0.003, 0.024}	$\Xi^* J/\psi(4630)$	
		4621.7	{-0.700, -0.198, -0.167, -0.605, -0.205, -0.035, -0.136, -0.123}		
		4728.5	{0.157, -0.625, 0.561, 0.075, -0.492, -0.090, -0.111, -0.046}		
		4787.6	{0.479, -0.330, -0.051, -0.578, 0.480, -0.306, 0.010, -0.001}		
		4902.2	{-0.434, -0.484, -0.013, 0.479, 0.564, -0.174, 0.007, 0.004}		
		$\frac{3}{2}^-$	4413.7	{-0.042, 0.058, 0.119, -0.038, -0.001, -0.003, -0.990}	$\Xi J/\psi(4415)$
			4509.4	{-0.141, 0.018, 0.008, 0.100, -0.020, -0.985, 0.007}	$\Xi^*\eta_c(4517)$
4614.5	{0.548, -0.582, -0.350, 0.469, 0.041, -0.047, -0.118}				
4630.6	{-0.027, -0.034, -0.007, 0.073, -0.996, 0.031, -0.004}		$\Xi^* J/\psi(4630)$		
4715.2	{0.374, 0.804, -0.363, 0.284, -0.015, -0.013, -0.023}				
4769.1	{-0.460, -0.091, -0.849, -0.226, 0.006, 0.034, -0.079}				
4819.0	{-0.570, 0.033, 0.0998, 0.795, 0.077, 0.162, 0.007}				
$\frac{5}{2}^-$	4631.7		{-0.006, 0.99998}	$\Xi^* J/\psi(4630)$	
	4790.0	{0.99998, 0.006}			

TABLE X. The partial width ratios for the hidden charm decays of the $ssnc\bar{c}$ pentaquark states. The masses are all in units of MeV.

J^P	Mass	$\Xi^* J/\psi$	$\Xi^*\eta_c$	$\Xi J/\psi$	$\Xi\eta_c$
$\frac{1}{2}^-$	4573.4	0		1	1.8
	4621.7	0		1	1.02
	4728.5	0.38		1	0.20
	4787.6	1		0.001	0.00003
	4902.2	1		0.002	0.0006
$\frac{3}{2}^-$	4614.5	0	0.11	1	
	4715.2	0.23	0.26	1	
	4769.1	0.004	0.16	1	
	4819.0	1	5.7	0.01	
$\frac{5}{2}^-$	4790.0	1			

TABLE XI. The partial width ratios for the $ssc\otimes n\bar{c}$ open charm decays of the $ssnc\bar{c}$ pentaquark states. The masses are all in units of MeV.

J^P	Mass	$\Omega_c^*\bar{D}^*$	$\Omega_c^*\bar{D}$	$\Omega_c\bar{D}^*$	$\Omega_c\bar{D}$
$\frac{1}{2}^-$	4573.4	0		0	1
	4621.7	0		0	1
	4728.5	0		2.5	1
	4787.6	0.10		3.9	1
	4902.2	46.0		4.6	1
$\frac{3}{2}^-$	4614.5	0	0	0	
	4715.2	0	1	10.3	
	4769.1	0	1	0.72	
	4819.0	2.1	1	0.33	
$\frac{5}{2}^-$	4790.0	1			

These wave functions have definite symmetry under the exchange of the first two quarks. $(q_1q_2)_1^6$ and $(q_1q_2)_0^3$ are symmetric, while $(q_1q_2)_1^3$ and $(q_1q_2)_0^6$ are antisymmetric.

Next we consider the flavor wave function. Taking the Pauli principle into account, we can obtain four types of total wave functions.

1. Type A [Flavor = $\{(nnsQ\bar{Q})^{I=1}, ssnQ\bar{Q}\}$]:

(a) $J^P = 1/2^-$:

$$\begin{aligned}\Psi_{A1}^{1/2} &= q_1q_2q'_3Q_4\bar{Q}_5 \otimes \beta_3^{1/2}, \\ \Psi_{A2}^{1/2} &= q_1q_2q'_3Q_4\bar{Q}_5 \otimes \beta_5^{1/2}, \\ \Psi_{A3}^{1/2} &= q_1q_2q'_3Q_4\bar{Q}_5 \otimes \beta_6^{1/2}, \\ \Psi_{A4}^{1/2} &= q_1q_2q'_3Q_4\bar{Q}_5 \otimes \beta_7^{1/2},\end{aligned}$$

TABLE XII. The partial width ratios for the $nsc\otimes s\bar{c}$ open charm decays of the $ssnc\bar{c}$ pentaquark states. The masses are all in units of MeV.

J^P	Mass	$\Xi_c^* \bar{D}_s^*$	$\Xi_c^* \bar{D}_s$	$\Xi_c' \bar{D}_s^*$	$\Xi_c' \bar{D}_s$	$\Xi_c \bar{D}_s^*$	$\Xi_c \bar{D}_s$
$\frac{1}{2}^-$	4573.4	0	0	1	0	0.003	
	4621.7	0	0	0.0005	1	28.1	
	4728.5	0	15.3	1	67.4	5.9	
	4787.6	0.04	3.0	1	0.09	0.0009	
$\frac{3}{2}^-$	4902.2	42.4	5.0	1	0.06	0.19	
	4614.5	0	1	0	14.5		
	4715.2	0	1	35.9	31.5		
	4769.1	12.9	1	1.7	14.9		
$\frac{5}{2}^-$	4819.0	1.0	1	0.29	2.2		
	4790.0	1					

TABLE XIII. Pentaquark masses and eigenvectors of the $sssc\bar{c}$ systems. The masses are all in units of MeV.

System	J^P	Mass	Eigenvector	Scattering state
$sssc\bar{c}$	$\frac{1}{2}^-$	4736.0	{0.164, -0.386, 0.908}	$\Omega J/\psi(4769)$
		4894.4	{0.756, -0.542, -0.367}	
		5009.4	{0.633, 0.747, 0.203}	
$\frac{3}{2}^-$	$\frac{3}{2}^-$	4645.1	{-0.190, -0.021, -0.982}	$\Omega\eta_c(4656)$
		4767.5	{-0.082, -0.996, 0.037}	$\Omega J/\psi(4769)$
		4924.1	{0.978, -0.087, -0.187}	
$\frac{5}{2}^-$	$\frac{5}{2}^-$	4768.6	{1}	$\Omega J/\psi(4769)$

TABLE XIV. The partial width ratios for the hidden charm decays of the $sssc\bar{c}$ pentaquark states. The masses are all in units of MeV.

J^P	Mass	$\Omega J/\psi$	$\Omega\eta_c$
$\frac{1}{2}^-$	4894.4	1	
	5009.4	1	
$\frac{3}{2}^-$	4924.1	1	6.1

TABLE XV. The partial width ratios for the open charm decays of the $sssc\bar{c}$ pentaquark states. The masses are all in units of MeV.

J^P	Mass	$\Omega_c^* \bar{D}_s^*$	$\Omega_c^* \bar{D}_s$	$\Omega_c \bar{D}_s^*$	$\Omega_c \bar{D}_s$
$\frac{1}{2}^-$	4894.4	0.01	1	0.2	
	5009.4	10.2	1	0.2	
$\frac{3}{2}^-$	4924.1	4.3	3.3	1	

$$\begin{aligned}
\Psi_{A5}^{1/2} &= q_1 q_2 q'_3 Q_4 \bar{Q}_5 \otimes \beta_9^{1/2}, \\
\Psi_{A6}^{1/2} &= q_1 q_2 q'_3 Q_4 \bar{Q}_5 \otimes \beta_{11}^{1/2}, \\
\Psi_{A7}^{1/2} &= q_1 q_2 q'_3 Q_4 \bar{Q}_5 \otimes \beta_{12}^{1/2}, \\
\Psi_{A8}^{1/2} &= q_1 q_2 q'_3 Q_4 \bar{Q}_5 \otimes \beta_{14}^{1/2},
\end{aligned} \tag{A4}$$

(b) $J^P = 3/2^-$:

$$\begin{aligned}
\Psi_{A1}^{3/2} &= q_1 q_2 q'_3 Q_4 \bar{Q}_5 \otimes \beta_4^{3/2}, \\
\Psi_{A2}^{3/2} &= q_1 q_2 q'_3 Q_4 \bar{Q}_5 \otimes \beta_5^{3/2}, \\
\Psi_{A3}^{3/2} &= q_1 q_2 q'_3 Q_4 \bar{Q}_5 \otimes \beta_6^{3/2}, \\
\Psi_{A4}^{3/2} &= q_1 q_2 q'_3 Q_4 \bar{Q}_5 \otimes \beta_7^{3/2}, \\
\Psi_{A5}^{3/2} &= q_1 q_2 q'_3 Q_4 \bar{Q}_5 \otimes \beta_9^{3/2}, \\
\Psi_{A6}^{3/2} &= q_1 q_2 q'_3 Q_4 \bar{Q}_5 \otimes \beta_{10}^{3/2}, \\
\Psi_{A7}^{3/2} &= q_1 q_2 q'_3 Q_4 \bar{Q}_5 \otimes \beta_{11}^{3/2},
\end{aligned} \tag{A5}$$

(c) $J^P = 5/2^-$:

$$\begin{aligned}
\Psi_{A1}^{5/2} &= q_1 q_2 q'_3 Q_4 \bar{Q}_5 \otimes \beta_2^{5/2}, \\
\Psi_{A2}^{5/2} &= q_1 q_2 q'_3 Q_4 \bar{Q}_5 \otimes \beta_3^{5/2},
\end{aligned} \tag{A6}$$

2. Type B [Flavor = $(nnsQ\bar{Q})^{I=0}$]:

(a) $J^P = 1/2^-$:

$$\begin{aligned}
\Psi_{B1}^{1/2} &= q_1 q_2 q'_3 Q_4 \bar{Q}_5 \otimes \beta_1^{1/2}, \\
\Psi_{B2}^{1/2} &= q_1 q_2 q'_3 Q_4 \bar{Q}_5 \otimes \beta_2^{1/2}, \\
\Psi_{B3}^{1/2} &= q_1 q_2 q'_3 Q_4 \bar{Q}_5 \otimes \beta_4^{1/2}, \\
\Psi_{B4}^{1/2} &= q_1 q_2 q'_3 Q_4 \bar{Q}_5 \otimes \beta_8^{1/2}, \\
\Psi_{B5}^{1/2} &= q_1 q_2 q'_3 Q_4 \bar{Q}_5 \otimes \beta_{10}^{1/2}, \\
\Psi_{B6}^{1/2} &= q_1 q_2 q'_3 Q_4 \bar{Q}_5 \otimes \beta_{13}^{1/2}, \\
\Psi_{B7}^{1/2} &= q_1 q_2 q'_3 Q_4 \bar{Q}_5 \otimes \beta_{15}^{1/2},
\end{aligned} \tag{A7}$$

(b) $J^P = 3/2^-$:

$$\begin{aligned}
\Psi_{B1}^{3/2} &= q_1 q_2 q'_3 Q_4 \bar{Q}_5 \otimes \beta_1^{3/2}, \\
\Psi_{B2}^{3/2} &= q_1 q_2 q'_3 Q_4 \bar{Q}_5 \otimes \beta_2^{3/2}, \\
\Psi_{B3}^{3/2} &= q_1 q_2 q'_3 Q_4 \bar{Q}_5 \otimes \beta_3^{3/2}, \\
\Psi_{B4}^{3/2} &= q_1 q_2 q'_3 Q_4 \bar{Q}_5 \otimes \beta_8^{3/2}, \\
\Psi_{B5}^{3/2} &= q_1 q_2 q'_3 Q_4 \bar{Q}_5 \otimes \beta_{12}^{3/2},
\end{aligned} \tag{A8}$$

(c) $J^P = 5/2^-$:

$$\Psi_{B1}^{5/2} = q_1 q_2 q'_3 Q_4 \bar{Q}_5 \otimes \beta_1^{5/2}, \tag{A9}$$

3. Type C [Flavor = $\{(nmmQ\bar{Q})^{I=3/2}, sssQ\bar{Q}\}$]:

$$(a) J^P = 1/2^-: \quad + [n_1 n_2] n_3 Q_4 \bar{Q}_5 \otimes \beta_{15}^{1/2}), \quad (A13)$$

$$\begin{aligned} \Psi_{C1}^{1/2} &= q_1 q_2 q_3 Q_4 \bar{Q}_5 \otimes \frac{1}{\sqrt{2}} \left(\beta_3^{1/2} - \beta_7^{1/2} \right), \\ \Psi_{C2}^{1/2} &= q_1 q_2 q_3 Q_4 \bar{Q}_5 \otimes \frac{1}{\sqrt{2}} \left(\beta_5^{1/2} - \beta_9^{1/2} \right), \\ \Psi_{C3}^{1/2} &= q_1 q_2 q_3 Q_4 \bar{Q}_5 \otimes \beta_{11}^{1/2}, \end{aligned} \quad (A10)$$

$$(b) J^P = 3/2^-: \quad \Psi_{C1}^{3/2} = q_1 q_2 q_3 Q_4 \bar{Q}_5 \otimes \frac{1}{\sqrt{2}} \left(\beta_4^{3/2} - \beta_7^{3/2} \right),$$

$$\Psi_{C2}^{3/2} = q_1 q_2 q_3 Q_4 \bar{Q}_5 \otimes \beta_9^{3/2},$$

$$\Psi_{C3}^{3/2} = q_1 q_2 q_3 Q_4 \bar{Q}_5 \otimes \beta_{10}^{3/2}, \quad (A11)$$

$$(c) J^P = 5/2^-: \quad \Psi_{C1}^{5/2} = q_1 q_2 q_3 Q_4 \bar{Q}_5 \otimes \beta_3^{5/2}, \quad (A12)$$

4. Type D [Flavor = $(nnnQ\bar{Q})^{I=1/2}$]:

$$(a) J^P = 1/2^-: \quad \Psi_{D1}^{1/2} = \frac{1}{\sqrt{2}} \left(\{n_1 n_2\} n_3 Q_4 \bar{Q}_5 \otimes \beta_6^{1/2} \right.$$

$$\left. - [n_1 n_2] n_3 Q_4 \bar{Q}_5 \otimes \beta_1^{1/2} \right),$$

$$\Psi_{D2}^{1/2} = \frac{1}{2} \left[\{n_1 n_2\} n_3 Q_4 \bar{Q}_5 \otimes \left(\beta_3^{1/2} + \beta_7^{1/2} \right) \right.$$

$$\left. + [n_1 n_2] n_3 Q_4 \bar{Q}_5 \otimes \left(\beta_2^{1/2} - \beta_8^{1/2} \right) \right],$$

$$\Psi_{D3}^{1/2} = \frac{1}{2} \left[\{n_1 n_2\} n_3 Q_4 \bar{Q}_5 \otimes \left(\beta_5^{1/2} + \beta_9^{1/2} \right) \right.$$

$$\left. + [n_1 n_2] n_3 Q_4 \bar{Q}_5 \otimes \left(\beta_4^{1/2} - \beta_{10}^{1/2} \right) \right],$$

$$\Psi_{D4}^{1/2} = \frac{1}{\sqrt{2}} \left(\{n_1 n_2\} n_3 Q_4 \bar{Q}_5 \otimes \beta_{12}^{1/2} \right.$$

$$\left. + [n_1 n_2] n_3 Q_4 \bar{Q}_5 \otimes \beta_{13}^{1/2} \right),$$

$$\Psi_{D5}^{1/2} = \frac{1}{\sqrt{2}} \left(\{n_1 n_2\} n_3 Q_4 \bar{Q}_5 \otimes \beta_{14}^{1/2} \right.$$

$$(b) J^P = 3/2^-: \quad \Psi_{D1}^{3/2} = \frac{1}{\sqrt{2}} \left(\{n_1 n_2\} n_3 Q_4 \bar{Q}_5 \otimes \beta_5^{3/2} \right.$$

$$\left. - [n_1 n_2] n_3 Q_4 \bar{Q}_5 \otimes \beta_1^{3/2} \right),$$

$$\Psi_{D2}^{3/2} = \frac{1}{\sqrt{2}} \left(\{n_1 n_2\} n_3 Q_4 \bar{Q}_5 \otimes \beta_6^{3/2} \right.$$

$$\left. - [n_1 n_2] n_3 Q_4 \bar{Q}_5 \otimes \beta_2^{3/2} \right),$$

$$\Psi_{D3}^{3/2} = \frac{1}{2} \left[\{n_1 n_2\} n_3 Q_4 \bar{Q}_5 \otimes \left(\beta_4^{3/2} + \beta_7^{3/2} \right) \right.$$

$$\left. + [n_1 n_2] n_3 Q_4 \bar{Q}_5 \otimes \left(\beta_3^{3/2} - \beta_8^{3/2} \right) \right],$$

$$\Psi_{D4}^{3/2} = \frac{1}{\sqrt{2}} \left(\{n_1 n_2\} n_3 Q_4 \bar{Q}_5 \otimes \beta_{11}^{3/2} \right.$$

$$\left. + [n_1 n_2] n_3 Q_4 \bar{Q}_5 \otimes \beta_{12}^{3/2} \right), \quad (A14)$$

$$(c) J^P = 5/2^-: \quad \Psi_{D1}^{5/2} = \frac{1}{\sqrt{2}} \left(\{n_1 n_2\} n_3 Q_4 \bar{Q}_5 \otimes \beta_2^{5/2} \right.$$

$$\left. - [n_1 n_2] n_3 Q_4 \bar{Q}_5 \otimes \beta_1^{5/2} \right), \quad (A15)$$

where $\{n_1 n_2\} \equiv (n_1 n_2)^{I=1}$ and $[n_1 n_2] \equiv (n_1 n_2)^{I=0}$.

Appendix B: The eigenvectors of the pentaquarks

To obtain the relative widths of pentaquark decays into a light baryon and a charmonium, or into a charm baryon and an anticharm meson, one needs to transform the eigenvectors to the corresponding configuration. We transform the eigenvectors of $qqqc\bar{c}$ pentaquark states into all possible configurations, as shown in Tables **XVI–XX**. Since we are only interested in the OZI-superallowed decays, we only present the color-singlet components.

-
- [1] M. Gell-Mann, *Phys. Lett.* **8**, 214 (1964).
[2] G. Zweig, *DEVELOPMENTS IN THE QUARK THEORY OF HADRONS. VOL. 1. 1964 - 1978*, *Developments in the Quark Theory of Hadrons*, Volume 1. Edited by D. Lichtenberg and S. Rosen. pp. 22-101, 22 (1964).
[3] R. L. Jaffe, *Phys. Rev.* **D15**, 267 (1977).
[4] R. L. Jaffe, *Phys. Rev.* **D15**, 281 (1977).
[5] H.-M. Chan and H. Høgaasen, *Phys. Lett.* **72B**, 121 (1977).
[6] K.-T. Chao, *Nucl. Phys.* **B169**, 281 (1980).
[7] K.-T. Chao, *Nucl. Phys.* **B183**, 435 (1981).
[8] K.-T. Chao, *Z. Phys.* **C7**, 317 (1981).
[9] M. Fukugita, K. Konishi, and T. H. Hansson, *Phys. Lett.* **74B**, 261 (1978).
[10] H. Høgaasen and P. Sorba, *Nucl. Phys.* **B145**, 119 (1978).
[11] D. Strottman, *Phys. Rev.* **D20**, 748 (1979).
[12] S. K. Choi *et al.* (Belle Collaboration), *Phys. Rev. Lett.* **91**, 262001 (2003), arXiv:hep-ex/0309032 [hep-ex].
[13] D. Acosta *et al.* (CDF Collaboration), *Phys. Rev. Lett.* **93**, 072001 (2004), arXiv:hep-ex/0312021 [hep-ex].
[14] V. M. Abazov *et al.* (D0 Collaboration), *Phys. Rev. Lett.* **93**, 162002 (2004), arXiv:hep-ex/0405004 [hep-ex].
[15] B. Aubert *et al.* (BABAR Collaboration), *Phys. Rev.* **D71**, 071103 (2005), arXiv:hep-ex/0406022 [hep-ex].

TABLE XVI. The eigenvectors of the $nnnc\bar{c}$ pentaquark states. The masses are all in units of MeV.

I	J^P	Mass	$nnn\otimes c\bar{c}$				$nnc\otimes n\bar{c}$						
			$\Delta J/\psi$	$\Delta\eta_c$	NJ/ψ	$N\eta_c$	$\Sigma_c^*\bar{D}^*$	$\Sigma_c^*\bar{D}$	$\Sigma_c\bar{D}^*$	$\Sigma_c\bar{D}$	$\Lambda_c\bar{D}^*$	$\Lambda_c\bar{D}$	
$\frac{3}{2}$	$\frac{1}{2}^-$	4601.9	-0.197				0.146		-0.563	0.304			
		4717.1	0.114				-0.621		-0.218	-0.081			
	$\frac{3}{2}^-$	4633.0	-0.053	-0.118			-0.521	0.350	-0.211				
$\frac{1}{2}$	$\frac{1}{2}^-$	4327.0			0.084	-0.134		-0.075	0.060	0.566	-0.326	0.029	
		4372.4			0.093	0.077		0.322	0.380	0.067	0.072	-0.426	
		4480.9			-0.069	-0.035		-0.403	0.357	0.115	0.364	0.087	
	$\frac{3}{2}^-$	4367.4			-0.072			0.030	-0.555	-0.036		-0.364	
		4476.3			-0.011			0.124	0.119	0.602		-0.230	
		4524.5			0.056			0.560	0.181	-0.231		-0.210	
		$\frac{5}{2}^-$	4546.0					0.667					

TABLE XVII. The eigenvectors for the $(nmsc\bar{c})^{I=1}$ pentaquark states. The masses are all in units of MeV.

J^P	Mass	$nns\otimes c\bar{c}$				$nnc\otimes s\bar{c}$				$nsc\otimes n\bar{c}$					
		Σ^*J/ψ	$\Sigma^*\eta_c$	$\Sigma J/\psi$	$\Sigma\eta_c$	$\Sigma_c^*\bar{D}_s^*$	$\Sigma_c^*\bar{D}_s$	$\Sigma_c\bar{D}_s^*$	$\Sigma_c\bar{D}_s$	$\Xi_c^*\bar{D}^*$	$\Xi_c^*\bar{D}$	$\Xi_c'\bar{D}^*$	$\Xi_c'\bar{D}$	$\Xi_c\bar{D}^*$	$\Xi_c\bar{D}$
$\frac{1}{2}^-$	4442.8	0.144		0.134	-0.190	-0.124	0.206	0.856		-0.089	0.356	0.156	-0.050	0.269	
	4522.2	-0.008		-0.105	-0.108	-0.476	-0.631	0.004		-0.169	0.038	-0.447	-0.254	0.221	
	4612.6	0.138		-0.106	-0.034	-0.664	0.545	-0.004		-0.195	-0.360	-0.076	0.300	0.136	
	4696.3	0.229		0.017	-0.005	-0.017	0.396	-0.238		0.164	-0.181	0.130	-0.624	0.259	
	4808.1	-0.140		-0.012	-0.007	0.525	0.188	0.071		-0.666	-0.134	-0.098	-0.160	-0.041	
$\frac{3}{2}^-$	4485.9	0.789	-0.053	0.072		0.030	0.688	0.283		0.040	0.046	-0.265		-0.003	
	4488.4	0.610	0.023	-0.091		-0.007	-0.517	0.001		-0.082	-0.446	0.138		-0.344	
	4584.9	-0.022	-0.021	0.054		-0.009	0.046	-0.907		0.078	-0.022	-0.439		-0.230	
	4636.2	-0.016	-0.048	-0.062		-0.924	-0.098	0.068		-0.257	-0.177	-0.245		0.268	
	4728.8	-0.062	-0.132	0.004		-0.302	0.301	-0.153		0.602	-0.343	0.245		0.116	
$\frac{5}{2}^-$	4644.3	-0.006				0.940				0.473					

- [16] R. Aaij *et al.* (LHCb Collaboration), *Eur. Phys. J.* **C72**, 1972 (2012), [arXiv:1112.5310 \[hep-ex\]](#).
- [17] S. Chatrchyan *et al.* (CMS Collaboration), *JHEP* **04**, 154 (2013), [arXiv:1302.3968 \[hep-ex\]](#).
- [18] M. Ablikim *et al.* (BESIII Collaboration), *Phys. Rev. Lett.* **112**, 092001 (2014), [arXiv:1310.4101 \[hep-ex\]](#).
- [19] K. Abe *et al.* (Belle Collaboration), *Proceedings, 32nd International Conference on High Energy Physics (ICHEP 2004): Beijing, China, August 16-22, 2004. Vol. 1+2*, *Phys. Rev. Lett.* **94**, 182002 (2005), [arXiv:hep-ex/0408126 \[hep-ex\]](#).
- [20] T. Aaltonen *et al.* (CDF Collaboration), *Phys. Rev. Lett.* **102**, 242002 (2009), [arXiv:0903.2229 \[hep-ex\]](#).
- [21] B. Aubert *et al.* (BaBar Collaboration), *Phys. Rev. Lett.* **95**, 142001 (2005), [arXiv:hep-ex/0506081 \[hep-ex\]](#).
- [22] B. Aubert *et al.* (BaBar Collaboration), *Proceedings of the 33rd International Conference on High Energy Physics (ICHEP '06): Moscow, Russia, July 26-August 2, 2006*, *Phys. Rev. Lett.* **98**, 212001 (2007), [arXiv:hep-ex/0610057 \[hep-ex\]](#).
- [23] X. L. Wang *et al.* (Belle Collaboration), *Phys. Rev. Lett.* **99**, 142002 (2007), [arXiv:0707.3699 \[hep-ex\]](#).
- [24] E. S. Swanson, *Phys. Lett.* **B588**, 189 (2004), [arXiv:hep-ph/0311229 \[hep-ph\]](#).
- [25] F.-K. Guo, C. Hanhart, U.-G. Meiner, Q. Wang, Q. Zhao, and B.-S. Zou, *Rev. Mod. Phys.* **90**, 015004 (2018), [arXiv:1705.00141 \[hep-ph\]](#).
- [26] S.-L. Zhu, *Phys. Lett.* **B625**, 212 (2005), [arXiv:hep-ph/0507025 \[hep-ph\]](#).
- [27] A. Esposito, A. Pilloni, and A. D. Polosa, *Phys. Lett.* **B758**, 292 (2016), [arXiv:1603.07667 \[hep-ph\]](#).
- [28] Y. Cui, X.-L. Chen, W.-Z. Deng, and S.-L. Zhu, *HEP* **NP** **31**, 7 (2007), [arXiv:hep-ph/0607226 \[hep-ph\]](#).

TABLE XVIII. The eigenvectors for the $(nnsc\bar{c})^{I=0}$ pentaquark states. The masses are all in units of MeV.

J^P	Mass	$nns\otimes c\bar{c}$		$nnc\otimes s\bar{c}$		$nsc\otimes n\bar{c}$					
		$\Lambda J/\psi$	$\Lambda\eta_c$	$\Lambda_c\bar{D}_s^*$	$\Lambda_c\bar{D}_s$	$\Xi_c^*\bar{D}^*$	$\Xi_c^*\bar{D}$	$\Xi_c'\bar{D}^*$	$\Xi_c'\bar{D}$	$\Xi_c\bar{D}^*$	$\Xi_c\bar{D}$
$\frac{1}{2}^-$	4197.4	0.652	-0.059	-0.089	0.795	0.028		-0.028	0.340	-0.105	-0.061
	4208.6	-0.735	-0.057	-0.009	0.234	0.104		0.047	0.417	0.208	-0.371
	4386.6	0.095	-0.078	-0.894	-0.006	-0.031		-0.343	-0.184	0.267	-0.188
	4465.0	-0.091	0.132	0.103	-0.015	-0.084		-0.354	0.311	0.344	0.548
	4489.6	-0.112	-0.096	-0.052	0.474	0.404		0.318	-0.320	0.336	0.251
	4607.0	0.076	0.041	-0.365	-0.089	-0.484		0.537	0.148	0.191	0.104
$\frac{3}{2}^-$	4387.3	-0.031		-0.865		-0.094	0.197	-0.446		0.213	
	4501.5	-0.077		-0.253		-0.036	0.631	0.433		-0.212	
	4603.6	-0.006		-0.236		-0.174	-0.189	-0.169		-0.738	
	4656.0	-0.065		0.204		0.675	0.234	-0.319		-0.178	
$\frac{5}{2}^-$	4680.6					0.817					

TABLE XIX. The eigenvectors for the $ssnc\bar{c}$ pentaquark states. The masses are all in units of MeV.

J^P	Mass	$ssn\otimes c\bar{c}$				$ssc\otimes n\bar{c}$				$nsc\otimes s\bar{c}$					
		$\Xi^* J/\psi$	$\Xi^*\eta_c$	$\Xi J/\psi$	$\Xi\eta_c$	$\Omega_c^*\bar{D}^*$	$\Omega_c^*\bar{D}$	$\Omega_c\bar{D}^*$	$\Omega_c\bar{D}$	$\Xi_c^*\bar{D}_s^*$	$\Xi_c^*\bar{D}_s$	$\Xi_c'\bar{D}_s^*$	$\Xi_c'\bar{D}_s$	$\Xi_c\bar{D}_s^*$	$\Xi_c\bar{D}_s$
$\frac{1}{2}^-$	4573.4	0.068		-0.171	0.199	0.112		-0.180	-0.725	-0.038		0.065	0.426	-0.397	0.017
	4621.7	-0.035		-0.136	-0.123	-0.426		-0.526	-0.078	0.246		0.312	0.003	0.135	-0.492
	4728.5	-0.091		-0.111	-0.046	-0.542		0.401	0.158	0.335		-0.298	-0.052	-0.447	-0.112
	4787.6	-0.306		0.010	-0.001	0.164		-0.653	0.260	0.085		-0.534	0.247	0.075	-0.007
	4902.2	-0.174		0.007	0.004	0.673		0.191	0.078	0.602		0.187	0.074	0.019	0.030
$\frac{3}{2}^-$	4614.5	0.041	-0.047	-0.118		-0.012	-0.751	-0.065		-0.047	0.410	0.042		0.449	
	4715.2	-0.015	-0.013	-0.023		0.096	0.162	0.848		-0.101	-0.053	-0.447		0.276	
	4769.1	0.006	0.034	-0.079		-0.702	-0.310	0.313		0.486	0.070	-0.109		-0.257	
	4819.0	0.077	0.162	0.007		0.665	-0.323	0.208		0.445	-0.330	0.200		0.090	
$\frac{5}{2}^-$	4790.0	0.006				0.945				-0.469					

TABLE XX. The eigenvectors for the $sss\bar{c}$ pentaquark states. The masses are all in units of MeV.

J^P	Mass	$sss\otimes c\bar{c}$		$ssc\otimes s\bar{c}$			
		$\Omega J/\psi$	$\Omega\eta_c$	$\Omega_c^*\bar{D}_s^*$	$\Omega_c^*\bar{D}_s$	$\Omega_c\bar{D}_s^*$	$\Omega_c\bar{D}_s$
$\frac{1}{2}^-$	4894.4	-0.367		0.098		-0.582	0.226
	5009.4	0.203		-0.628		-0.176	-0.072
$\frac{3}{2}^-$	4924.1	-0.087	-0.187	-0.531	0.327	-0.203	

- [29] W. Park and S. H. Lee, *Nucl. Phys.* **A925**, 161 (2014), [arXiv:1311.5330 \[nucl-th\]](#).
[30] R. F. Lebed, R. E. Mitchell, and E. S. Swanson, *Prog. Part. Nucl. Phys.* **93**, 143 (2017), [arXiv:1610.04528 \[hep-ph\]](#).

- [31] A. Esposito, A. Pilloni, and A. D. Polosa, *Phys. Rept.* **668**, 1 (2017), [arXiv:1611.07920 \[hep-ph\]](#).
[32] H.-X. Chen, W. Chen, X. Liu, and S.-L. Zhu, *Phys. Rept.* **639**, 1 (2016), [arXiv:1601.02092 \[hep-ph\]](#).
[33] A. Ali, J. S. Lange, and S. Stone, *Prog. Part. Nucl. Phys.* **97**, 123 (2017), [arXiv:1706.00610 \[hep-ph\]](#).
[34] Y.-R. Liu, H.-X. Chen, W. Chen, X. Liu, and S.-L. Zhu, *Prog. Part. Nucl. Phys.* **107**, 237 (2019), [arXiv:1903.11976 \[hep-ph\]](#).
[35] R. Aaij *et al.* (LHCb Collaboration), *Phys. Rev. Lett.* **115**, 072001 (2015), [arXiv:1507.03414 \[hep-ex\]](#).
[36] R. Aaij *et al.* (LHCb Collaboration), *Phys. Rev. Lett.* **122**, 222001 (2019), [arXiv:1904.03947 \[hep-ex\]](#).
[37] R. Chen, X. Liu, X.-Q. Li, and S.-L. Zhu, *Phys. Rev. Lett.* **115**, 132002 (2015), [arXiv:1507.03704 \[hep-ph\]](#).

- [38] H.-X. Chen, W. Chen, X. Liu, T. G. Steele, and S.-L. Zhu, *Phys. Rev. Lett.* **115**, 172001 (2015), [arXiv:1507.03717 \[hep-ph\]](#).
- [39] H. Huang, C. Deng, J. Ping, and F. Wang, *Eur. Phys. J.* **C76**, 624 (2016), [arXiv:1510.04648 \[hep-ph\]](#).
- [40] U.-G. Meißner and J. A. Oller, *Phys. Lett.* **B751**, 59 (2015), [arXiv:1507.07478 \[hep-ph\]](#).
- [41] L. Roca, J. Nieves, and E. Oset, *Phys. Rev.* **D92**, 094003 (2015), [arXiv:1507.04249 \[hep-ph\]](#).
- [42] K. Azizi, Y. Sarac, and H. Sundu, *Phys. Rev.* **D95**, 094016 (2017), [arXiv:1612.07479 \[hep-ph\]](#).
- [43] R. Chen, X. Liu, and S.-L. Zhu, *Nucl. Phys.* **A954**, 406 (2016), [arXiv:1601.03233 \[hep-ph\]](#).
- [44] H.-X. Chen, E.-L. Cui, W. Chen, X. Liu, T. G. Steele, and S.-L. Zhu, *Eur. Phys. J.* **C76**, 572 (2016), [arXiv:1602.02433 \[hep-ph\]](#).
- [45] R. Chen, Z.-F. Sun, X. Liu, and S.-L. Zhu, *Phys. Rev.* **D100**, 011502 (2019), [arXiv:1903.11013 \[hep-ph\]](#).
- [46] H.-X. Chen, W. Chen, and S.-L. Zhu, (2019), [arXiv:1903.11001 \[hep-ph\]](#).
- [47] F.-K. Guo, H.-J. Jing, U.-G. Meiner, and S. Sakai, *Phys. Rev.* **D99**, 091501 (2019), [arXiv:1903.11503 \[hep-ph\]](#).
- [48] J. He, *Eur. Phys. J.* **C79**, 393 (2019), [arXiv:1903.11872 \[hep-ph\]](#).
- [49] M.-Z. Liu, Y.-W. Pan, F.-Z. Peng, M. Sánchez Sánchez, L.-S. Geng, A. Hosaka, and M. Pavon Valderrama, *Phys. Rev. Lett.* **122**, 242001 (2019), [arXiv:1903.11560 \[hep-ph\]](#).
- [50] R. F. Lebed, *Phys. Lett.* **B749**, 454 (2015), [arXiv:1507.05867 \[hep-ph\]](#).
- [51] L. Maiani, A. D. Polosa, and V. Riquer, *Phys. Lett.* **B749**, 289 (2015), [arXiv:1507.04980 \[hep-ph\]](#).
- [52] A. Mironov and A. Morozov, *JETP Lett.* **102**, 271 (2015), [*Pisma Zh. Eksp. Teor. Fiz.*102,no.5,302(2015)], [arXiv:1507.04694 \[hep-ph\]](#).
- [53] Z.-G. Wang, *Eur. Phys. J.* **C76**, 70 (2016), [arXiv:1508.01468 \[hep-ph\]](#).
- [54] R. Zhu and C.-F. Qiao, *Phys. Lett.* **B756**, 259 (2016), [arXiv:1510.08693 \[hep-ph\]](#).
- [55] E. Santopinto and A. Giachino, *Phys. Rev.* **D96**, 014014 (2017), [arXiv:1604.03769 \[hep-ph\]](#).
- [56] J. M. Richard, A. Valcarce, and J. Vijande, *Phys. Lett.* **B774**, 710 (2017), [arXiv:1710.08239 \[hep-ph\]](#).
- [57] A. Ali and A. Ya. Parkhomenko, *Phys. Lett.* **B793**, 365 (2019), [arXiv:1904.00446 \[hep-ph\]](#).
- [58] Y. Ne'eman, *Nucl. Phys.* **26**, 222 (1961), [,34(1961)].
- [59] M. Gell-Mann, *Phys. Rev.* **125**, 1067 (1962).
- [60] E. Eichten, K. Gottfried, T. Kinoshita, K. D. Lane, and T.-M. Yan, *Phys. Rev.* **D17**, 3090 (1978), [Erratum: *Phys. Rev.D* 21, 313 (1980)].
- [61] A. De Rújula, H. Georgi, and S. L. Glashow, *Phys. Rev.* **D12**, 147 (1975).
- [62] N. Isgur and G. Karl, *Phys. Lett.* **72B**, 109 (1977).
- [63] J. L. Basdevant and S. Boukraa, *Z. Phys.* **C28**, 413 (1985).
- [64] S. Godfrey and N. Isgur, *Phys. Rev. D* **32**, 189 (1985).
- [65] S. Capstick and N. Isgur, *Proceedings, International Conference on Hadron Spectroscopy: College Park, Maryland, April 20-22, 1985*, *Phys. Rev.* **D34**, 2809 (1986), [*AIP Conf. Proc.*132,267(1985)].
- [66] Y. B. Zeldovich and A. D. Sakharov, *Yad. Fiz.* **4**, 395 (1966).
- [67] Y. B. Zeldovich and A. D. Sakharov, *Sov. J. Nucl. Phys.* **4**, 283 (1967).
- [68] T. A. DeGrand, R. L. Jaffe, K. Johnson, and J. E. Kiskis, *Phys. Rev.* **D12**, 2060 (1975).
- [69] Y. Cui, X.-L. Chen, W.-Z. Deng, and S.-L. Zhu, *Phys. Rev.* **D73**, 014018 (2006), [arXiv:hep-ph/0511150 \[hep-ph\]](#).
- [70] F. Buccella, H. Hogaasen, J.-M. Richard, and P. Sorba, *Eur. Phys. J.* **C49**, 743 (2007), [arXiv:hep-ph/0608001 \[hep-ph\]](#).
- [71] J. Wu, Y.-R. Liu, K. Chen, X. Liu, and S.-L. Zhu, *Phys. Rev.* **D95**, 034002 (2017), [arXiv:1701.03873 \[hep-ph\]](#).
- [72] M. Karliner, S. Nussinov, and J. L. Rosner, *Phys. Rev.* **D95**, 034011 (2017), [arXiv:1611.00348 \[hep-ph\]](#).
- [73] H. Høgaasen, E. Kou, J.-M. Richard, and P. Sorba, *Phys. Lett.* **B732**, 97 (2014), [arXiv:1309.2049 \[hep-ph\]](#).
- [74] H.-M. Chan, M. Fukugita, T. H. Hansson, H. J. Hoffman, K. Konishi, H. Hogaasen, and S. T. Tsou, *Phys. Lett.* **76B**, 634 (1978).
- [75] X.-Z. Weng, X.-L. Chen, and W.-Z. Deng, *Phys. Rev.* **D97**, 054008 (2018), [arXiv:1801.08644 \[hep-ph\]](#).
- [76] R. Aaij *et al.* (LHCb Collaboration), *Phys. Rev. Lett.* **119**, 112001 (2017), [arXiv:1707.01621 \[hep-ex\]](#).
- [77] H. Høgaasen, J. M. Richard, and P. Sorba, *Phys. Rev.* **D73**, 054013 (2006), [arXiv:hep-ph/0511039 \[hep-ph\]](#).
- [78] L. Zhao, W.-Z. Deng, and S.-L. Zhu, *Phys. Rev.* **D90**, 094031 (2014), [arXiv:1408.3924 \[hep-ph\]](#).
- [79] C. Gao, *Group Theory and its Application in Particle Physics (in Chinese)* (Higher Education Press, 1992).